This is a non-peer reviewed preprint submitted to EarthArXiv on 7 October 2023

Coral geochemical response to uplift in the aftermath of the 2005 Nias-Simeulue earthquake

Sindia M. Sosdian[1,2*], Michael K. Gagan[2,3,4], Danny H. Natawidjaja[5], Bambang W. Suwargadi[6], Hamdi Rifai[7], Dudi Prayudi[6], Imam Suprihanto[6], Heather Scott-Gagan[2], Wahyoe S. Hantoro[6,†]

[1]School of Earth and Ocean Sciences, Cardiff University, Cardiff, CF10 3AT, United Kingdom
[2]Research School of Earth Sciences, The Australian National University, Canberra, ACT 2601, Australia
[3]School of Earth, Atmospheric and Life Sciences, University of Wollongong, Wollongong, NSW 2522, Australia
[4]School of Earth and Environmental Sciences, The University of Queensland, St Lucia, QLD 4072, Australia
[5]Research Center for Geological Disaster, National Research and Innovation Agency (BRIN), Bandung 40135, Indonesia
[6]Research Center for Geotechnology, Indonesian Institute of Sciences (LIPI), Bandung 40135, Indonesia
[7]Department of Physics, Universitas Negeri Padang, Padang 25131, Indonesia
[†]Deceased

*Corresponding author: sosdians@cardiff.ac.uk

ABSTRACT

On 28 March 2005, the Indonesian islands of Nias and Simeulue experienced a powerful M_w 8.6 earthquake and widespread co-seismic uplift and subsidence. In areas of coastal uplift (up to ~2.8 m), fringing reef coral communities were killed by exposure, while deeper corals that survived were subjected to habitats with altered runoff, sediment and nutrient regimes. Here we present time-series (2000–2009) of Ba/Ca, Mn/Ca, and Y/Ca variability in massive *Porites* corals from Nias to assess the environmental impact of a wide range of vertical displacement (+2.5 m to -0.4 m). High-resolution LA-ICP-MS measurements show that skeletal Mn/Ca increased at uplifted sites, regardless of reef type, indicating a post-earthquake increase in suspended sediment delivery. Transient and/or long-term increases in skeletal Y/Ca at all uplift sites support the idea of increased sediment delivery. Coral Ba/Ca and Mn/Ca in lagoonal environments highlight the additional influences of reef bathymetry, wind-driven sediment resuspension, and phytoplankton blooms on coral geochemistry. Together, the results show that the Nias reefs adapted to fundamentally altered hydrographic conditions. Our findings indicate that centuries of repeated subsidence and uplift during great-earthquake cycles along the Sunda megathrust have shaped the life-cycle, species composition and resilience of the West Sumatran coral reefs.

Introduction

Tectonic activity along subduction zones produces the most powerful earthquakes observed on Earth. One example of these megathrust earthquakes is the 2004 Indonesian Great Boxing Day earthquake which devastated infrastructure and human lives in 14 countries. Beyond the impact on society, these events have sudden and lingering impacts such as vertical displacement (i.e. uplift, subsidence) and tsunamis which wreak havoc on coastal zones and coral reef systems. Unprecedented within the life-span of coral reefs, these abrupt co-seismic disturbances and concomitant environmental changes play a major role in shaping coasts and the speciation and distribution of reef-building scleractinian corals (Stoddart, 1972; Briggs et al. 2006; Foster et al. 2006; Taylor et al. 2008; McAdoo et al. 2008; Taylor, 2011). For example, subduction zone earthquakes can raise shallow coral reef communities above sea level and lead to their demise by aerial exposure with loss in range of suitable habitat (Stoddart, 1972; Briggs et al. 2006; Foster et al. 2006; Taylor et al. 2008; McAdoo et al. 2008; Taylor, 2011). Shifts to distinct new reef zones with altered environment conditions (i.e. light, turbidity) can encourage colonization by filamentous algae and physiological stress (Stoddart, 1972; van Woesik, 1996; Ito et al. 2020).

Co-seismic landslides and tsunami-related effects associated with earthquakes increase sediment delivery to coastal reefs and alter biogeochemical conditions (Cortes et al. 1992; Dadson et al. 2004; Jaffe et al. 2006; Searle, 2006; Albert et al 2007; Hovius et al. 2011). Long-term impacts result in migration and recolonization of impacted habitats and shifts in marine foundation species and species community structure (Aronson et al. 2012; Sepulveda & Valdivia, 2016; Chunga-Llauce & Pacheco, 2021; Thomsen et al. 2021). Indeed, long-term patterns in tropical Indo-Pacific coral reef biodiversity are tied to tectonic activity (Keith et al. 2013; Leprieur et al. 2016; Miahljevic et al. 2017).

The Sunda megathrust, a 5500 km long subduction-zone fault west of Sumatra, Indonesia, produces great-earthquakes about every two centuries (Sieh et al. 2008) with the potential to shape the coastal environment and coral reef communities across large spatial scales (Fig. 1). Powerful megathrust earthquakes occurred in December 2004 (M_w 9.1) and three months later in March 2005 (M_w 8.6) centered near the offshore islands of Simeulue and Nias, resulting in significant uplift (+2.8 m) and tsunami damage (Foster et al. 2006; Briggs et al. 2006). Co-seismic uplift during both earthquakes led to extensive reef mortality and corals from deeper habitats entered the reef flat zone altering the ecological dynamics of fringing reef ecosystems (Foster et al. 2006). Vertical displacement changing the coastal geomorphology and distribution and movement of sediment in the nearshore environment, including loss of intertidal habitats minimizing the buffering capacity of this system (Foster et al. 2006).

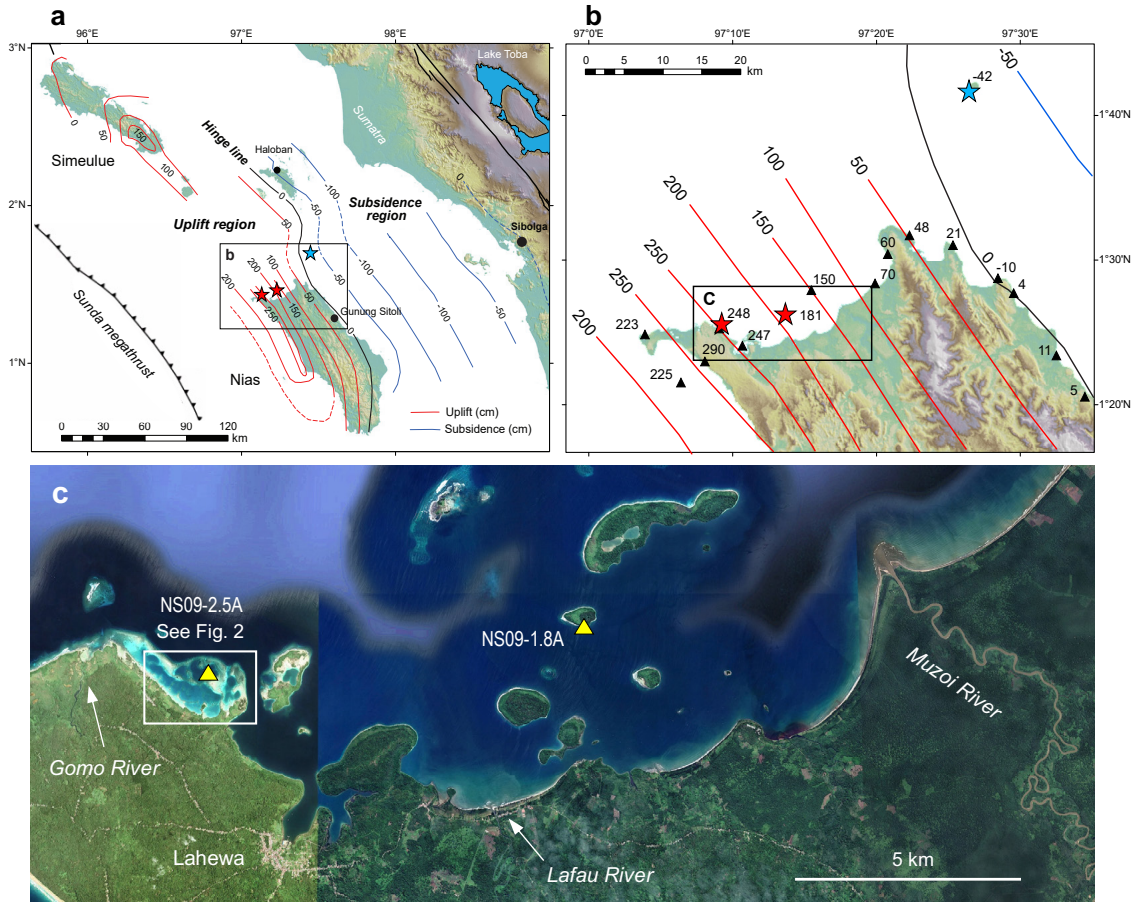

Figure 1. Attributes of the study area. (**a**) Location of Nias, the Sunda megathrust and coseismic uplift and subsidence for the 28 March 2005 Nias-Simeulue earthquake (after Briggs et al. 2006) (**b**) Location of coral drill-sites NS09-2.5A and NS09-1.8A (red stars) and NS09-M0.4A (blue star) within the pattern of coseismic uplift and subsidence. Map contours are in centimetres, based on analysis of coral microatoll elevations (triangles, after Briggs et al. 2006). Site locations include uplift (2.5 m, 1.8 m) and subsidence (-0.4 m). (**c**) Location of the 2.5A and 1.8A uplift sites relative to riverine suspended sediment sources. 1.8A is in proximity (~7 km) to the largest river (Muzoi), and also a smaller river (Lafau). 2.5A is proximal (~3 km) to a small river (Gomo). Map image is for December 2022 on Google Earth Pro 7.3.6.9345 (2022 version) at http://www.google.com/earth/index.html (accessed August 6, 2023).

Despite the potential impact of earthquakes in these coral reef systems there is a lack of information on relevant spatial and temporal timescales. Instrumental data documenting these instantaneous events and their impacts are limited to continuous GPS data to document co-seismic motion (Briggs et al. 2006). Also, most environmental assessments to date are visual and provide only a snapshot of reef conditions, water quality and health post-earthquake on a scale of days to months (Cortese et al. 1997; Foster et al. 2006; Searle, 2006). Observations are needed to provide knowledge of environmental change pre- and post-earthquake and potential interaction between land displacement, coastal hydrographic conditions, and coral reef communities on short and long-timescales.

Long-lived *Porites sp.* corals inhabit these tectonically active regions and experience recurring amounts of uplift and subsidence and associated environmental stress over time. *Porites* corals can live for 100s of years, and those that remain submerged after earthquake events provide an archive of earthquake-induced environmental change and coral physiological response. For instance, the growth response of *Porites* microatolls has provided a record of interseismic and co-seismic crustal motion with an ~200 y recurrence cycle along the Sunda megathrust (Zachariasen et al. 1999; Natawidjaja et al. 2006; Sieh et al. 2008; Meltzner et al. 2012, 2015). Although the isotopic and elemental compositions of *Porites* skeletons have been shown to track past environmental change (Druffel 1997; Gagan et al. 2000; Saha et al. 2016), their application in earthquake prone regions is limited. Recent work has shown that shifts in skeletal carbon-isotope ratios in *Porites* reflect changes in light exposure following co-seismic vertical displacements during the 2005 Nias-Simeulue earthquake (Gagan et al. 2015; Ito et al. 2020). Also, Mg/Ca has been linked to tsunami-induced algal blooms and/or presence of endolithic algae (Ito et al. 2020). However, to date, there are no coral records that characterize post-earthquake marine geochemical change in coral reef settings.

Records of Ba, Mn, and Y in coral skeletons have the potential to provide information on earthquake related changes in sediment delivery to nearshore areas and associated shifts in sediment dynamics within reef environments. Delivery of sediments via runoff to the coastal zone is the primary source for these elements in nearshore regions (Shen et al. 1991). These coral proxy records have been widely used to reconstruct terrigenous runoff on seasonal and longer timescales in the tropics (Saha et al. 2016). For instance, Ba/Ca in corals reflects changes in Ba in the surface-ocean reef environment related to a range of processes such as upwelling (Yamazaki et al. 2011; Walther et al. 2013), river discharge (McCulloch et al. 2003; Fleitmann et al. 2007), wind/wave associated sediment resuspension (Esslemont et al. 2004) and primary productivity and barite formation (Saha et al. 2018). Mn/Ca in corals has been shown to track Mn cycling associated with large erosive events and delivery of suspended particulate matter through riverine discharge (Alibert et al. 2003; Moyer et al. 2012; Inoue et al. 2014). The residence of Y in the estuarine zone is longer and gradual release and recycling of Y implies coral Y/Ca will record longer-term changes in dissolved Y concentrations related to environmental perturbations (Wyndham et al. 2004*;* Lewis et al. 2007, 2012, 2018; Saha et al. 2018; Leonard et al. 2019) such as major terrestrial runoff changes or episodes of large scale erosion.

Here we present the first coral records of Ba/Ca, Mn/Ca, and Y/Ca as evidence of environmental shifts in reef systems in the aftermath of the great Nias-Simeulue earthquake of 28 March 2005. Maximum vertical displacement was centered on the northwest coast of Nias (+2.8 m), while a trough of subsidence (to -1.1 m) occurred between the island and mainland Sumatra (see Figure 1b after Briggs et al. 2006). We explore ~9-year-long geochemical records for six massive *Porites* corals positioned along a transect of vertical displacement from +2.5 m uplift to -0.4 subsidence (Fig. 1), and across different reef environments (e.g., lagoonal, fringing). We showcase the potential for Ba/Ca, Mn/Ca and Y/Ca to geochemically fingerprint shifts in sediment dynamics and reef environment following the earthquake. The new geochemical records, along with information about great-earthquake recurrence intervals, allow us to assess the long-term environmental impact of vertical tectonic motion on coral reef expansion and retreat in earthquake prone regions.

Study site and coral drilling

Nias is located ~125 km offshore of the west Sumatran coast (1° N, 97.5° E) and experiences an equatorial climate with abundant rainfall year-round (~4000 mm annual average). Situated in the Indo-Australian monsoon region, Nias experiences associated shifts in winds, generally from the northwest in boreal winter and southeast in boreal summer. Aperiodic variations in the Indian Ocean Dipole drive climate variability, with the positive mode marked by enhanced southeast winds, coastal upwelling and cooler SSTs, and reduced local rainfall (Saji et al. 1999). The island's terrain encompasses a mountainous inland area up to ~800 m in elevation surrounded by lowlands with dense vegetation. Rivers are perennially inundated leading to terrestrial discharge along coastal areas. A small concentration of rivers outflow along the northwest coast of Nias into the study area (Fig. 1). The dominant river is the Muzoi, with catchment headwaters extending ~40 km inland. Two smaller rivers, the Gomo and Lafau, have

localized coastal plain catchments.

During the 2005 earthquake, continuous global positioning station data and records of microatoll elevation were used to construct a contour map of co-seismic uplift and subsidence along the Nias coastline (Briggs et al. 2006). Four years after the earthquake, we used the pattern of tectonic deformation to guide the drilling of submerged, dome-shaped *Porites* corals in May 23-29, 2009 at three sites; two near the coast with strong uplift (+2.5 m, +1.8±0.16 m) and one offshore island control site with minor subsidence of -0.42±0.16 m (Table 1, Fig. 1). The +2.5 m collection site (2.5A) is located within a broad fringing reef lagoon on the northwest corner of Nias, with large areas of the reef exposed post-earthquake (Fig. 2), proximal to the small Gomo river outlet. The +1.8 m collection site (1.8A) is located 9 km to the east on the south side of Hilimakora Island, one of a series of small nearshore islands exposed to nearby runoff from the Muzoi and Lafau rivers. The control site, Sarangbaung Island (M0.4A), is located 20 km northeast of Nias, far from the influence of coastal rivers. The semi-diurnal tidal envelope along the coast of northwest Nias is microtidal with a maximum range of 1.2 m (Ito et al. 2020).

Table 1. Nias coral core information including environment description and age modelling approach. Age models are based on Gagan et al. (2015) $\delta^{13}C$ records for site 1.8A and a combination of Ba/Ca and coral core data for sites 2.5A and M0.4A.

Locality	Coral ID	Location	Vertical movement (m)	Environment	Extension rate (mm yr^{-1})	Earthquake tie point (mm)	Age model
Lahewa	NS09-2.5A-1	N 1°25'40.9", E 97°09'18.2"	+2.5	Reef lagoon	17	65	Ba/Ca cyclicity
Lahewa	NS09-2.5A-3	N 1°25'41.6", E 97°09'17.3"	+2.5	Reef lagoon	14	63	Ba/Ca cyclicity
Hilimakora island	NS09-1.8A-2	N 1°26'20.0", E 97°13'44.6"	+1.8	Fringing reef	16	66	$\delta^{13}C$ shift
Hilimakora island	NS09-1.8A-5	N 1°26'20.0", E 97°13'45.2"	+1.8	Fringing reef	18	77	$\delta^{13}C$ shift
Hilimakora island	NS09-1.8A-6	N 1°26'20.0", E 97°13'45.8"	+1.8	Fringing reef	18	74	$\delta^{13}C$ shift
Sarangbaung island	NS09-M0.4A-3	N 1°41'45.9", E 97°26'26.4"	- 0.4	Reef lagoon	17	59	Ba/Ca cyclicity

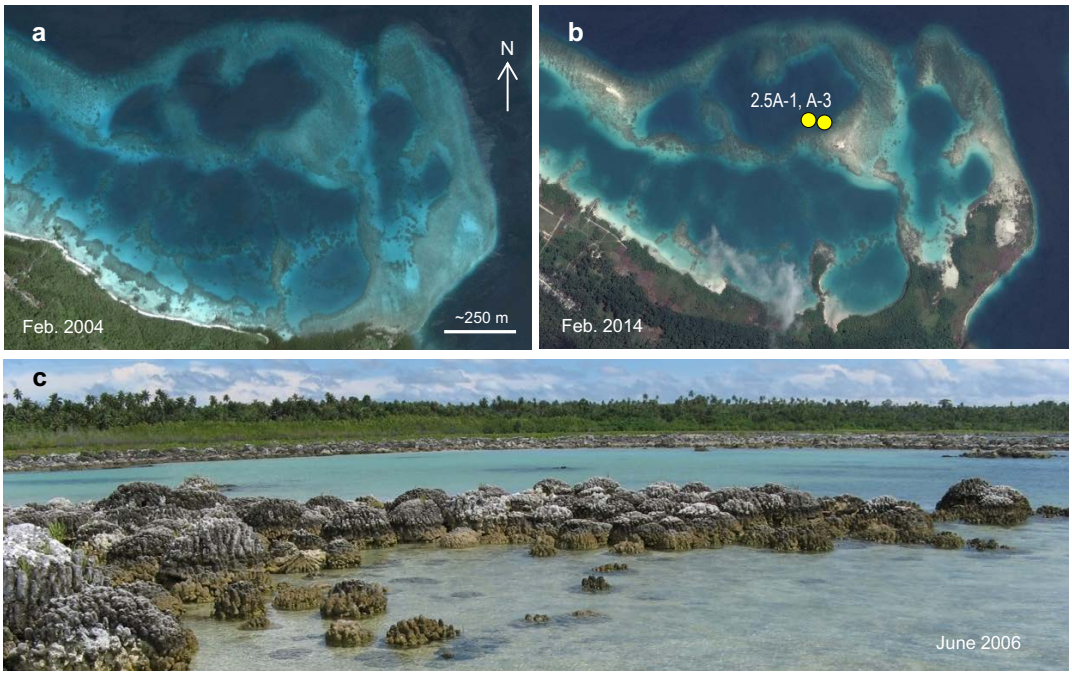

Figure 2. Images of coral drill-site 2.5A with the 2.5 m raised-reef lagoon. (**a**) Configuration of the deep-water lagoonal reef environment on 13 February 2004, about one year before the 28 March 2005 earthquake. (**b**) Raised reef on 17 February 2014 with exposure of new land and isolation of the shallowed lagoon due to 2.5 m of uplift. Yellow circles show locations of corals 2.5A-1 and 2.5A-3 drilled in May 2009. (**c**) 21 June 2006 image of raised *Porites sp.* corals that had colonized new seafloor created by interseismic subsidence prior to coseismic uplift. The *Porites*-dominated fringing reef exposed along the coast (background) is adjacent to shallow, turbid lagoonal water. Map images are on Google Earth Pro 7.3.6.9345 (2022 version) at http://www.google.com.earth/index.html (accessed July 13, 2023).

We analysed cores from healthy coral colonies drilled vertically to a depth of 50-70 cm from the upper growth surface in close proximity to each other at the 2.5A (two corals) and 1.8A (three corals) uplift sites, and from one coral at the M0.4A control site offshore (Fig. 1, Supplementary Fig. S1). Previous work has shown that average annual coral extension rates, based on annual cycles of $\delta^{13}C$ in coral skeleton that grew after the earthquake, and density band width in x-radiographs, range from 16 to 21 mm/y at the 1.8A and M0.4A sites (Gagan et al. 2015), which is typical for massive *Porites* colonies growing in warm tropical settings (Lough and Barnes 1997). In this study, we use annual cycles of Ba/Ca in coral skeleton that grew after the earthquake to estimate similar annual extension rates of 14 to 17 mm/y at the 2.5A and M0.4A sites (see Table 1, Supplementary Figs S2–S5 and Methods).

Results and discussion

Behaviour of coral Ba, Mn and Y in the aftermath of the 2005 earthquake

Here, we examine the pre- and post-earthquake signals in the new coral skeletal Ba/Ca, Mn/Ca and Y/Ca records. We explore the nature of post-earthquake changes in these elemental ratios and their links to altered environmental drivers, including terrestrial sediment delivery and reef-specific hydrographic factors (lagoon versus fringing reef).

Post-earthquake enhancement of sediment delivery

Average Mn/Ca values are highest at the 1.8A uplift site (1.2 umol/mol) under the influence of runoff from the Muzoi and Lafau rivers (Fig. 3). By comparison, Mn/Ca values are much lower at the 2.5A uplift site (0.6 umol/

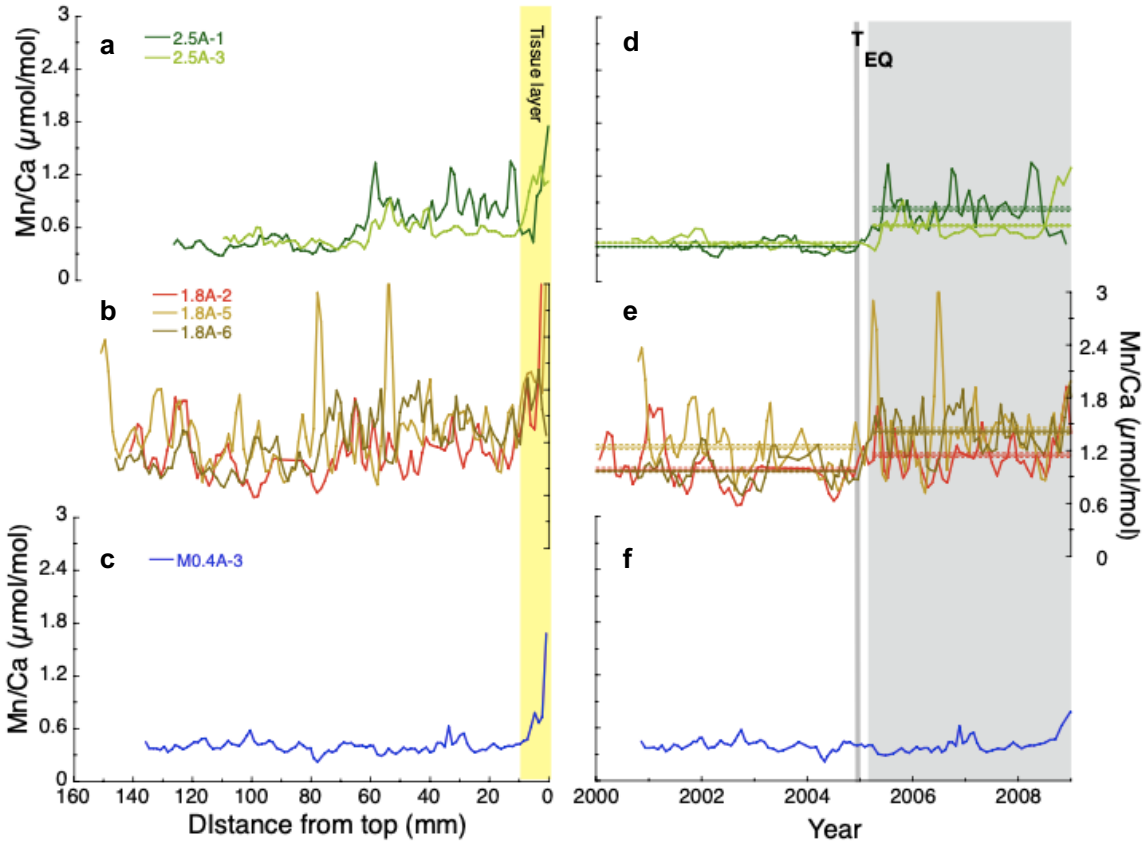

Figure 3. Coral Mn/Ca records before and after the March 2005 earthquake. Results are shown as 10-pt running means for the 2.5A and 1.8A uplift sites (**a, b, d, e**) and the M0.4A subsidence site (**c, f**) versus sampling distance from top of coral (on left) and time (on right**)**. Profiles with significant pre- and post-earthquake differences are indicated by their non-overlapping means (horizontal lines) with shaded 95% confidence envelopes (1.96 x standard error of the mean, see t-test results in Supplementary Table 1). Elemental data affected by coral tissue layer is indicated in yellow. Grey bar marks the timing of the December 2004 Indian Ocean tsunami. The interval following the March 2005 earthquake is highlighted by grey shading.

mol), proximal to the relatively small Gomo River. The lowest Mn/Ca values are recorded at the offshore subsidence site (M0.4A; 0.4 umol/mol) with no riverine influence. Mn/Ca values within these corals fall within the range for *Porites* at other locations (Lewis et al. 2018; Sayani et al. 2021). At the 2.5A uplift site, Mn/Ca shows sustained post-earthquake increases in both corals (A-1, A-3) of 0.43 and 0.20 µmol/mol, respectively (Fig. 3, $p<0.0001$ in Supplementary Table 1). Coral Mn/Ca at the 1.8A uplift site shows similar significant increases; 0.45 µmol/mol in coral A-6 and smaller increases of 0.17 and 0.18 µmol/mol in corals A-2 and A-5, respectively. In contrast, the M0.4A site shows negligible change in Mn/Ca (0.01 µmol/mol). Overall, these results indicate that mean Mn/Ca shows a significant increase at both uplift sites ranging from ~0.17 to 0.45 µmol /mol, regardless of reef environment.

We propose that the increase in Mn/Ca at both uplift sites is driven by a post-earthquake increase in sediment transport from land to sea. Earthquake and tsunami associated slope failure removes vegetation and facilitates increased erosion, sediment transport, and discharge during rainy events. Previous work in wet sub-tropical Taiwan has documented increases in sediment delivery to coastal environments following large earthquakes (Dadson et al. 2004; Hovius et al. 2011). The 2004 Boxing Day tsunami, which preceded the 2005 earthquake by three months, delivered waves up to 3.9 m in height at northwest Nias and left debris behind in trees (Jaffe et al. 2006), and would have made the land surface susceptible to erosion. Indeed, the 2005 earthquake mobilized sediment from the mountainous regions to the coast, so much so that alterations in beach profile led to an increase in available nearshore sediment supply (Foster et al. 2006). Overall, these findings indicate that earthquakes abruptly alter nearshore reefs with enhanced sediment delivery to coastal regions, and coral Mn/Ca provides a useful proxy to monitor earthquake-induced changes in suspended sediment load.

In addition to the changes in coral Mn/Ca, we document variations in coral Y/Ca associated with increased sediment delivery (Fig. 4). Corals A-2 and A-5 from the 1.8A uplift site, proximal to two rivers, have the highest

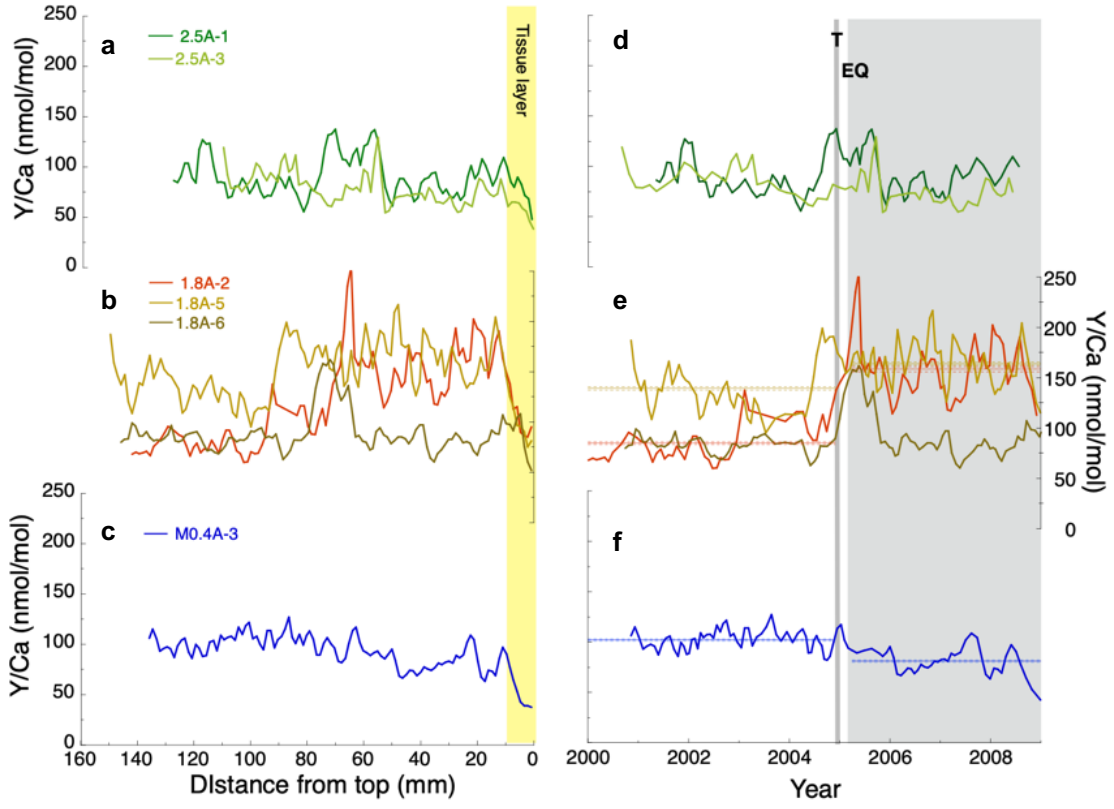

Figure 4. Coral Y/Ca records before and after the March 2005 earthquake. Results are shown as 10-pt running means for the 2.5A and 1.8A uplift sites (**a, b, d, e)** and the M0.4A subsidence site (**c, f**) versus sampling distance from top of coral (on left) and time (on right**)**. Profiles with significant pre- and post-earthquake differences are indicated by their non-overlapping means (horizontal lines) with shaded 95% confidence envelopes (1.96 x standard error of the mean, see t-test results in Supplementary Table 1). Elemental data affected by coral tissue layer is indicated in yellow. Grey bar marks the timing of the December 2004 Indian Ocean tsunami. The interval following the March 2005 earthquake is highlighted by grey shading.

mean Y/Ca values (136 nmol/mol), in contrast to locations with reduced (2.5A: 83 nmol/mol) or no influence of rivers (M0.4A: 91 nmol/mol) (Supplementary Table 1), in line with other studies showing gradients in Y/Ca with increasing riverine influence (Alibert et al. 2003; Lewis 2008). The range of values from these sites are similar to Y/Ca values previously reported for *Porites* in the Great Barrier Reef (83 nmol/mol, Lewis et al. 2018) and Puerto Rico (40 nmol/mol, Moyer et al. 2012). Y/Ca values at the 2.5A uplift site and M0.4A subsidence site are similar but are in contrast to the Mn/Ca data (i.e., lowest values at M0.4 site). The difference in Y/Ca and Mn/Ca values at these sites might reflect varying residence time of Mn and Y in the estuarine mixing zone (Lewis et al. 2018). Y/Ca at the 1.8A uplift site shows a statistically significant increase in corals A-2 and A-5, 74 and 25 nmol/mol, respectively (Fig. 4; $p<0.0001$ in Supplementary Table 1). Raised corals 1.8A-6, 2.5A-1 and 2.5A-3 show a prominent transient increase in Y/Ca around the time of the earthquake. The subsidence site coral M0.4A-3 shows no transient peak associated with the earthquake, but rather a long-term decrease in Y/Ca (26 nmol/mol).

Overall, the results for the two uplift sites show either a sustained post-earthquake increase in Y/Ca, or a transient increase in Y/Ca around the time of the earthquake. We suggest that signals are linked to increased sediment availability, as Y/Ca has been shown to record changes in suspended sediment on annual to longer timescales related to large erosion events *(*Alibert et al. 2003; Lewis et al. 2018*;* Leonard et al. 2019*)*. Indeed, during our initial visit to northwest Nias in June 2006, about 14 months after the earthquake, turbidity was particularly high in the +2.5 m raised-reef lagoon. Therefore, the tendency for transient increases in Y/Ca at the 2.5A lagoonal site could be due to tsunami, initially, followed by transient post-earthquake activation of the localised river sediment supply and wind-driven resuspension in the shallow lagoon. Additionally, during our initial visit to northwest Nias in June 2006, the *Porites* corals in the high uplift area offshore of Lahewa were coated with green-brown algae. Post-earthquake decomposition of algal mats and development of reducing conditions could contribute to the pulse like Y/Ca signature in cores at +1.8 and 2.5 m sites, similar to changes observed in western Sumatra during a red tide (Abram et al. 2003). Overall, the different nature of responses at the 1.8A uplift site, either transient or long term, suggests that within-reef differences in sediment availability and/or coral-colony specific factors could play a role in coral Y/Ca variability. The absence of a positive Y/Ca signal at the offshore subsidence site supports the idea of increased sediment activation specific to raised-reef sites. In sum, the Mn and Y records both suggest that nearshore suspended sediment availability expands in the aftermath of co-seismic uplift and alters the geochemical inventory of raised-reef environments in proximity to land.

Reef-specific earthquake-induced environmental changes

In addition to changes in sediment delivery associated with uplift, we propose that different types of reefs (e.g., fringing versus lagoonal) experience divergent patterns of post-earthquake environmental change, as evident from the Nias coral Mn/Ca and Ba/Ca records (Fig. 5). Skeletal Ba/Ca values for lagoonal sites (2.5A, M0.4A) show a seasonal cyclicity with average values (4.5-4.8 umol/mol) similar to those in *Porites* exposed to upwelling of Ba-enriched waters (Walther et al. 2013). In contrast, the coral Ba/Ca values for the 1.8A fringing reef site are lower on average (2.8-4.2 umol/mol), with annual peaks of varying intensity, similar to Ba/Ca records for sites proximal to rivers in Singapore with high suspended sediment loads (2-14 umol/mol, Tanzil et al. 2019). At the lagoonal sites, with uplift or subsidence, post-earthquake Ba/Ca increased on average by 0.18-0.24 umol/mol (Supplementary Table 1). At the fringing reef site 1.8A, Ba/Ca shows a variable response, including a significant post-earthquake decrease in coral A-6 and increases in corals A-2 and A-5.

These observations suggest that coral Ba/Ca has the potential to provide additional information about reef-specific impacts caused by the 2005 earthquake. In the wake of the 2004 tsunami, short-term increases in primary productivity (Sarangi et al. 2011; Haldar et al. 2013) could lead to pulse-like increases in Ba/Ca and Mn/Ca prior to the 2005 earthquake, followed by long-term increases in sediment resuspension and nutrients. Additionally, the 2.5A lagoonal site is proximal to a small river outlet, thus the long-term increase in coral Ba/Ca at this locality could be primarily driven by a mechanism specific to that reef. Distinct green-brown banding is present in the post-earthquake section of the site 2.5A drill-cores providing a visual indicator of earthquake-induced environmental stress and changes in primary productivity (Supplementary Figs S3 and S4; Gagan et al. 2015). Extensive shallowing of the raised-reef lagoon made the lagoon floor more susceptible to wind-induced sediment resuspension, and previous research has shown that accompanying release of sediment porewater nutrients drives algal blooms (Ogilvie and Mitchell 1998; Tenberg et al. 2003; Kalnejais et al. 2010). This increase in primary production would alter the Ba^{2+} inventory in the reef waters by barite formation, and resuspension of Ba-rich particles (Sinclair 2005; Saha et al. 2018).

Therefore, we propose that the post-earthquake increase in coral Ba/Ca at the +2.5m uplift site is related to increased lagoonal Ba^{2+} via wind-driven resuspension of Ba-rich particles, and partially to an increase in sediment delivery (Fig. 5). The sediment resuspension mechanism also could partly explain the increase in coral Mn/Ca at

the 2.5A lagoonal site given that decaying organic matter produces reducing condition leading to increases in porewater Mn^{2+} (Alibert et al. 2003; Wyndham et al. 2004). Thus the post-earthquake increase in Mn/Ca might be related to northwest wind-driven remobilization of sediment porewater Mn^{2+}, leading to seasonal increases in Mn^{2+} (Sayani et al. 2021). Along the same lines, we attribute the post-earthquake increase in coral Ba/Ca at the offshore subsidence site (M0.4A) to increased wave-penetration across the lowered reef-crest and sediment resuspension in the deepened lagoon. The 1.8A fringing reef site shows a variable Ba/Ca response and indicates that coral Ba/Ca at this site is influenced by local variations (i.e. sediment delivery) and/or coral-colony specific factors.

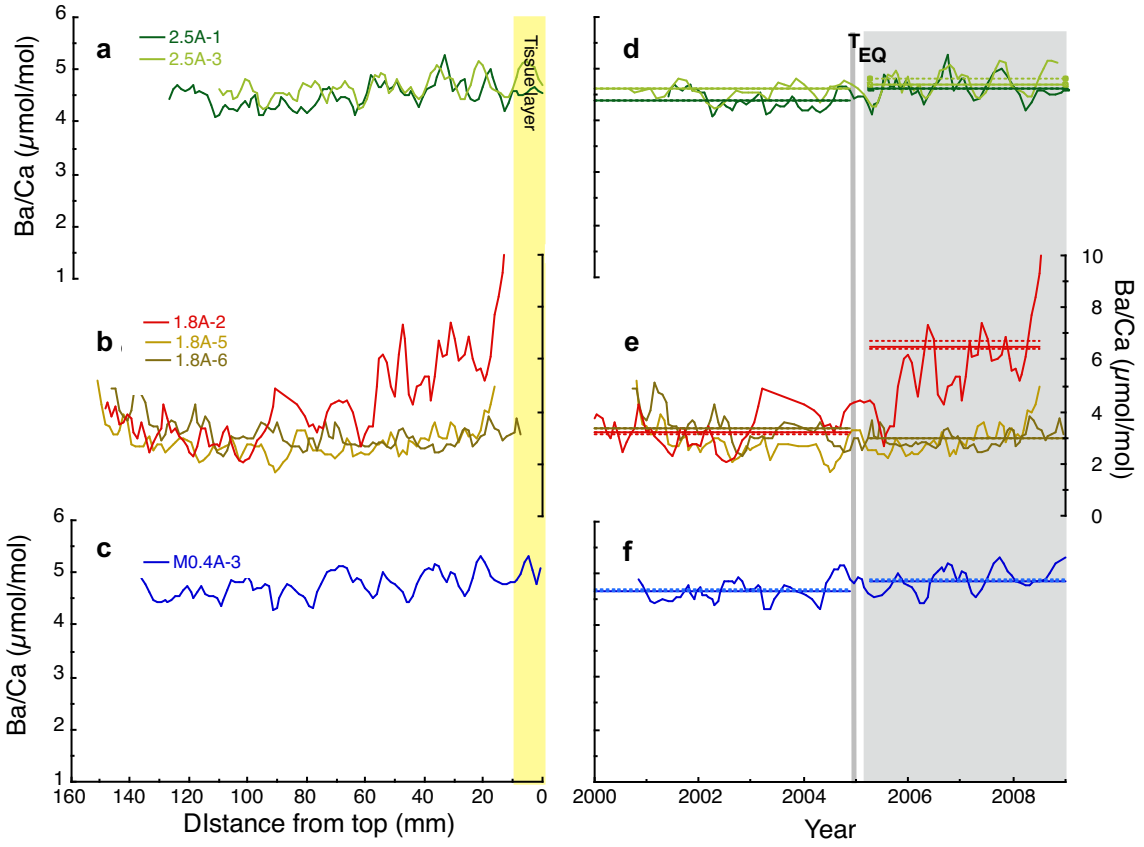

Figure 5. Coral Ba/Ca records before and after the March 2005 earthquake. Results are shown as 10-pt running means for the 2.5A and 1.8A uplift sites (**a, b, d, e)** and the M0.4A subsidence site (**c, f**) versus sampling distance from top of coral (on left) and time (on right**)**. Profiles with significant pre- and post-earthquake differences are indicated by their non-overlapping means (horizontal lines) with shaded 95% confidence envelopes (1.96 x standard error of the mean, see t-test results in Supplementary Table 1). Elemental data affected by coral tissue layer is indicated in yellow. Grey bar marks the timing of the December 2004 Indian Ocean tsunami. The interval following the March 2005 earthquake is highlighted by grey shading

Overall, these findings suggest that coral Mn/Ca, Ba/Ca and Y/Ca records in earthquake prone environments can provide information on sediment delivery and reef-specific environmental change associated with earthquake events. In the case of the 2005 earthquake in Nias, the sediment load of rivers in the co-seismically uplifted area evidently increased, and lagoonal reef settings, both raised and submerged, were impacted by wind- and wave-driven sediment resuspension and phytoplankton blooms. Taken together, these geochemical archives suggest that the pattern of co-seismic uplift and interseismic subsidence on the Sunda megathrust could set the pace of reef growth and retreat along the Mentawai Islands.

Coral reef response to great-earthquake cycles

The Nias coral geochemical records demonstrate that distinct environmental changes occurred in raised coral reef environments in the aftermath of the 2005 Nias-Simeulue earthquake. Our findings suggest that recurrent earthquake-induced environmental impacts contribute to periodic coral mortality, and may have shaped the coral

community structure, species composition and resilience of the West Sumatran coral reefs. The immediate loss of coral due to coseismic upheaval is evident, but the post-seismic environmental impacts could linger for years. For instance, prolonged periods of enhanced turbidity decrease light availability and negatively impact coral growth via reduced photosynthetic rates, with species-specific tolerance responses (Erftemeijer et al. 2012). Shifts in primary productivity can lead to infestations of endolithic algae, also with consequences for coral growth and survival (Ito et al. 2022). Further, alterations in depth habitat and physical disturbance associated with earthquakes and tsunami can impact coral cover patterns (Siringoringo et al. 2021).

Recent observational data for raised-reef sites along the northwest coast of Nias, including our study area, show a 50% decrease in live coral cover after the 2005 Nias-Simeulue earthquake (Siringoringo et al. 2021). The survey data document a shift from branching to massive growth-forms as the dominant surviving coral group due to the vulnerability of the branching morphology to physical damage. Recovery of the submerged sections of the raised reefs to pre-earthquake coral composition occurred within five years, but the process is dependent on environmental conditions, and full regeneration of coral community composition will clearly take longer. As a result, the predominance of stress-tolerant massive coral growth forms is evident in the coral communities along the length of the Sunda megathrust. Recent reef surveys show that the fringing coral reefs of Nias, Simeulue, and the Mentawai Islands are dominated by *Porites, Pavona* and *Psammocora,* which are mostly found with massive and sub-massive growth forms (Siringoringo et al. 2019).

Detailed studies of the growth-response of *Porites sp.* microatolls on the outer island arc of the Sunda megathrust have revealed a recurrent pattern of great-earthquake cycles over the last ~700 years, with century-scale periods of interseismic subsidence terminated by coseismic uplift (Natawidjaja et al. 2006; Sieh et al. 2008; Meltzner et al. 2015; Philibosian et al. 2017). Our analysis of the 2005 event indicates that interseismic subsidence promotes coral reef expansion, whereas coseismic upheaval leads to coral reef contraction. In northwest Nias, tectonic subsidence and reef expansion, via coral colonization of new seafloor, was well underway during the decades prior to the 2005 earthquake (Fig. 6). This observation is consistent with microatoll elevation data showing interseismic subsidence leading-in to 2005, and also before the 1861 Nias earthquake (Meltzner et al. 2015). Average interdecadal subsidence rates along the coast of northwest Nias were 7.2±5 mm/y before 1861 and 2.5-7.9 mm/y (site dependent) before 2005. These long intervals of interseismic quiescence provide stable environmental conditions where reefs can expand and thrive.

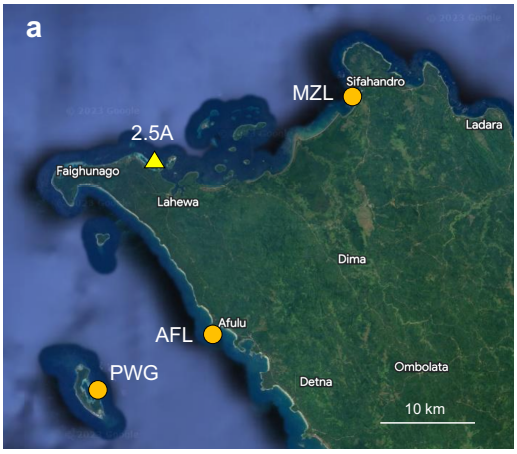

c	Rate of subsidence		
Site	Interseismic	Pre-1861 event	Pre-2005 event
AFL	7.0±5.0 mm/yr	10.7±8.0 mm/yr	7.9±2.0 mm/yr
PWG	3.5±2.1 mm/yr	8.5±2.5 mm/yr	
MZL		-4.41±2.1 mm/yr	2.5±3.0 mm/yr

Figure 6. Coral reef submergence and expansion in northwest Nias prior to megathrust earthquakes. (**a**) Location of coral drill-site 2.5A (this study) and coral microatoll records (AFL, PWG, MZL, Meltzner et al. 2015) that document interseismic subsidence prior to the 1861 and 2005 earthquakes. (**b)** 23 May 2009 image of *Porites sp.* corals at the 2.5A uplift site that colonized new seafloor created by subsidence before the March 2005 earthquake. Coral in foreground shows regrowth atop a dead *Porites sp.* colony that re-submerged during the decades leading-in to the 2005 earthquake. (**c)** Summary of subsidence rates in northwest Nias recorded by microatolls AFL, PWG and MZL prior to the 1861 and 2005 earthquakes. Subsidence increased during the decades immediately before the 1861 earthquake (Meltzner et al. 2015). Map image is for April 2023 on Google Earth Pro 7.3.9345 (2022 version) at http://www.google.com/earth/index.html (accessed June 15, 2023).

Following these periods of interseismic quiescence, geochemical reservoirs are suddenly transformed during great-earthquakes and entire reef ecosystems contract and adapt to environmental change in the aftermath. Figure 7 summarises the spatial and temporal histories of interseismic subsidence and coseismic uplift along the Sunda megathrust. We envisage a 3-phase reef-response within each great-earthquake cycle involving: (1) post-seismic coral reef contraction and adaptation; (2) slow century-scale sudsidence and equilibrium; and (3) reef expansion prior to the culminating earthquake (Sieh et al. 2008). However, the spatial and temporal status of the great-earthquake cycle varies in response to the tectonic status of specific sectors of the Sunda megathrust. For example, the Mentawai Islands sector has well-defined and regular earthquake cycles lasting ~200 years (Sieh et al. 2008; Philibosian et al. 2017). In contrast, the Batu Islands sector to the north is an unusual locality with long-term tectonic stability (Natawidjaja et al. 2004; Philibosian et al. 2014). The analysis also shows that the massive 2004 and 2005 earthquakes were the culminating events for the most recent earthquake cycle in the northern Sumatra-Andaman Island sector (Meltzner et al. 2012; 2015), and the reef adaptation process is presumably well underway. In contrast, the very recent rupture sequence in the Mentawai Islands sector is incomplete and raises the likelihood of further coral reef contraction and adaptation.

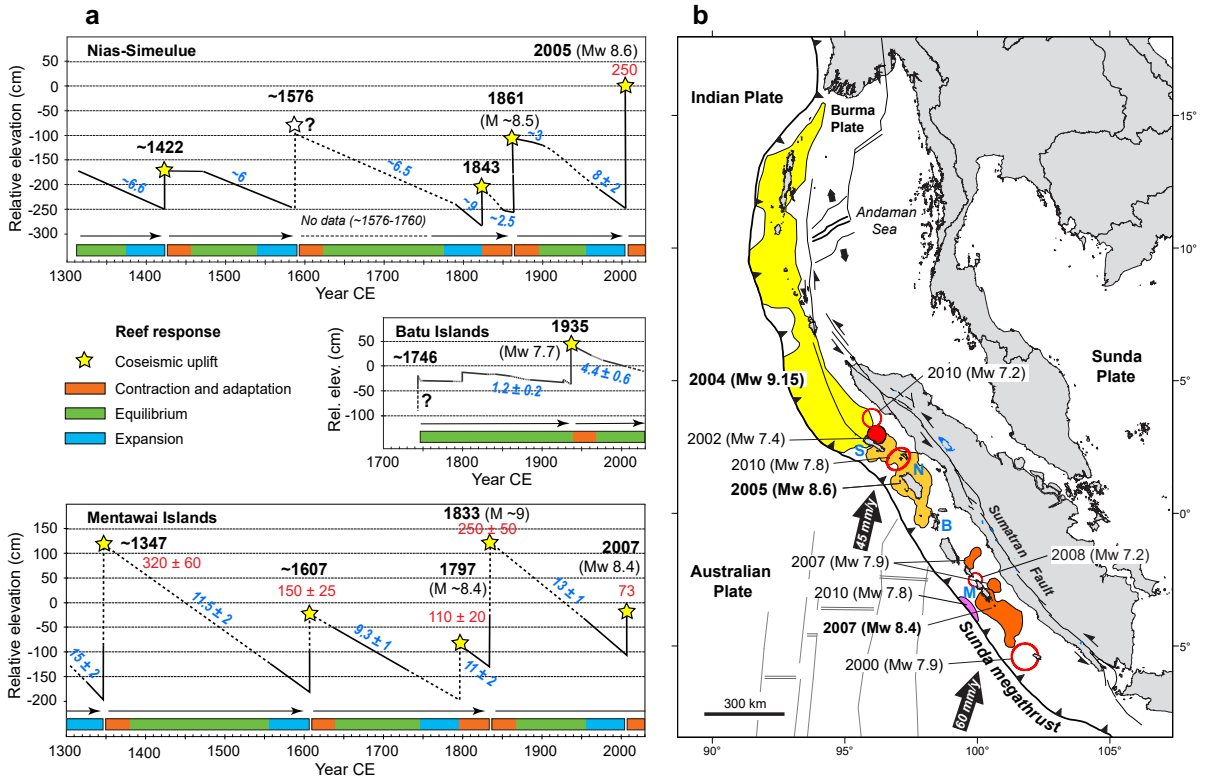

Figure 7. Temporal and spatial influence of great-earthquake cycles on coral reefs along the Sunda megathrust. (**a**) Schematic summary of earthquake cycles and coral reef response over the last seven centuries. Maximum coseismic uplift values are in red (±2σ) and interseismic subsidence rates are in blue (in mm/y, ±2σ); dotted lines are inferred. The Nias-Simeulue example is a composite microatoll elevation record for Simeulue (Bunon village, 1311–1576 CE, Meltzner et al. 2012) and northern Nias (sites AFL, MZL, PWG; 1800–1861 CE, 1960–2000 CE, Meltzner et al. 2015). Batu Islands is a composite for south Tanabala island showing a rare locality with long-term tectonic stability (Natawidjaja et al. 2004; Philibosian et al. 2014). Mentawai Islands shows strong earthquake cycles at Bulasat, South Pagai island (Sieh et al. 2008). The long periods of outer island arc subsidence promote reef expansion whereas culminating earthquakes cause reef contraction and adaptation. (**b**) Spatial distribution of crustal ruptures for recent large earthquakes (>Mw 7) along the Sunda megathrust since 2000 CE. Red circles indicate estimated rupture areas. Blue letters show the approximate locations of the earthquake cycle time-series for Nias-Simeulue (N, S), Batu Islands (B) and the Mentawai Islands (M). Map is adapted from Natawidjaja et al. (2006) with rupture areas and magnitudes from Briggs et al. (2006), Chlieh et al. (2007), Konca et al. (2008), Meltzner et al. (2010), Hill et al. (2012), and references therein.

Taken together, the available great-earthquake time-series suggest that the reef-response megacycle along the Sunda megathrust has recently entered a critical phase of coseismic risk, environmental upheaval and reef contraction and adaptation. Among the implications, our finding indicates that the tectonic status of the Sunda megathrust needs to be considered when evaluating the reef response to anthropogenic activity. As such, the island fringing reefs along most of Sunda megathrust appear to be at the cusp of an adaptational juncture that could last for decades. The near-culmination of the earthquake cycle creates an unusually dynamic spatial and temporal baseline of coral reef health against which to judge the effects of human agency on coral reefs.

Conclusions

Coral geochemical records from West Sumatra provide valuable archives of earthquake-induced shifts in coral reef environmental conditions. Specifically, skeletal Mn/Ca reflects changes in sediment delivery at uplifted reef sites, regardless of reef type, associated with the 2005 Nias-Simeulue earthquake. The increase in sediment delivery associated with the earthquake is tied to changes in riverine geomorphology and reef-specific changes brought about by vertical displacement. Skeletal Ba/Ca and Y/Ca support the idea of changes in sediment delivery to reef environments in the aftermath of earthquakes. Raised-reef lagoonal Ba/Ca and Mn/Ca records highlight the role of shoaling and changes in local hydrography on resuspension of sediments and primary productivity. Overall, these abrupt shifts in coral reef environments can alter the distribution of coral species and community structure of coral reefs. Our analysis of the 2005 event indicates that great-earthquake cycles along the Sunda megathrust have played a key role in shaping the modern distribution and homogeneity of coral species on the West Sumatran coral reefs, where lengthy periods of interseismic subsidence promote coral reef expansion, and coseismic upheaval leads to considerable demise. The observation of recurrent, century-scale reef-response megacycles in West Sumatra highlights the potential of subduction-zone tectonics in tropical regions to play a critical role in shaping coral reef systems. While our focus here is the Sunda megathrust, the reef-response megacycle concept could be applied to improve our understanding of island arc coral community status along subduction zone margins throughout the tropics.

Methods

Coral sample preparation and trace element analysis. Coral cores were longitudinally slabbed into 7-mm thick slices and X-rayed in order to identify a maximum growth axis and develop a basic chronology for each coral record (Supplementary Figs S2–S5). The slabs were cleaned using a hand-held ultrasonicator probe in Milli-Q water and dried overnight in an oven at 40°C. After removal of material for stable isotope analysis (see Gagan et al. 2015), a 25 x 95 mm (maximum) section was cut from the coral slice to fit within the sampling cell for analysis by laser ablation inductively coupled plasma mass spectrometry (LA-ICP-MS) at the Research School of Earth Sciences, the Australian National University. Each section was vigorously cleaned using the hand-held ultrasonicator in Milli-Q water and placed in an oven overnight to dry at 40°C. Laser scan-paths were selected to parallel the major growth axis of the coral and the stable isotope sampling path across at least eight years of coral growth to capture pre- and post-earthquake elemental variability.

The LA-ICP-MS laboratory procedures for analysis of trace elements in corals have been described by Sinclair et al. (1998), Fallon et al. (1999) and Wyndham et al. (2004). Briefly, the LA-ICP-MS system uses a 193 nm ArF excimer laser coupled to a Varian 820 ICP-MS to quantify trace element intensities. Ablated material was delivered to the ICP-MS via a mixed stream of Ar and He (Eggins et al. 1998). Prior to analysis, laser tracks were pre-ablated to remove surface contaminants using a large 100 um x 700 um rectangular spot, with the laser set at 20 Hz and 100 mJ. For the analytical work, ablation analysis was conducted in two consecutive traverses of the sample: major trace element analysis (Ba, Mn) using a 50 x 500 um spot size followed by trace element analysis (Y) using a 100 x 500 um spot size, as outlined in Wyndham et al (2004). The ablation analyses were carried out at a 40 um/s scan speed, 5 Hz repetition rate, 50 mJ energy, and using a 50% partially reflecting mirror. Measurements on standards were made at the beginning and end of each analysis section; the NIST 614 silicate glass certified reference material and an in-house pressed coral powder standard were used to normalize Y and Mn, and Ba, respectively (Fallon et al. 2002; Wyndham et al. 2004). The normalized data were smoothed with a 10-point averaging box filter to remove high frequency variation due to instrumental instability and counting statistics (Supplementary Figs S6–S8). All reported Y/Ca values are at least one order of magnitude greater than the detection limit (Wyndham et al. 2004).

We note that in some studies a stepwise pretreatment with intensive cleaning procedures (i.e., hydrogen peroxide rinses) has been employed for coral trace element analyses to ensure that the measured Mn and Y has substituted for Ca in the aragonite lattice, rather than reflecting organic phases or Mn oxide coatings (Lewis et al. 2007;

Kasper-Zubillaga et al. 2010; Inoue et al. 2014). We follow the method of Wyndham et al. (2004), which incorporates several pre-ablation steps to ensure minimal surface contamination. To assess the Mn signal we acquired Mn data from both analyses (major and trace element) along the same track in coral core 2.5A-1. We see similar post-earthquake increases in Mn in both analyses, which suggests the Mn signals are lattice bound (Supplementary Fig. S6). Also, there is a steep rise in Mn/Ca at the end of both records that is mostly restricted to skeletal elements that were surrounded with live coral tissue at the time of collection.

Coral core chronologies. We use the approach of Gagan et al. (2015) to generate age models for the three coral records at the 1.8A uplift site, and annual coral growth rates, coral core features, and coral Ba/Ca cyclicity were used to constrain the earthquake window for the 2.5A and M0.4 sites. Gagan et al. (2015) noted that the position of the step-change in skeletal $\delta^{13}C$ due to uplift or subsidence marks the position (and date) of the earthquake within each coral core at the 1.8A m and M0.4 sites. This 'chronological anchor point' was then used to estimate average coral extension rates. We rely on this approach to generate age models for the elemental records for the 1.8A fringing reef site. Gagan et al. (2015) noted that, in most cases, the position of the earthquake signal within the coral cores is marked by a slight change in skeletal density evident in X-radiographs, and estimated reasonable growth rates of 16-23 mm/y for the 1.8A corals.

While this approach is valid for the 1.8A site, at site 2.5A there is no clear signal in coral $\delta^{13}C$, presumably due to higher water column turbidity post-earthquake, which masked the effect of increased light intensity due to uplift (Gagan et al. 2015). Additionally, the juvenile coral M0.4A-3 does not show a distinct change (decrease) in $\delta^{13}C$ associated with subsidence and a decrease in light intensity, possibly due to ontogenetic effects (Gagan et al. 1996). In these cases, we use coral Ba/Ca cyclicity alongside skeletal density patterns in x-radiographs and coral core features to pinpoint the earthquake. At the 2.5A and M0.4 sites, coral Ba/Ca shows a distinct seasonal cyclicity, linked in other regions to seasonal upwelling (Yamazaki et al. 2011; Walther et al. 2013; Supplementary Figs S3–S5). We align high Ba/Ca peaks in the records to mid-October, around the end of the southeast monsoon when wind-driven upwelling and low sea surface temperatures reflect maximum shoaling of the thermocline (Horii et al. 2020), and low Ba/Ca peaks to mid-April, when upwelling is weak near the end of the northwest monsoon season.

Using this approach, the March 2005 earthquake event is at 59-63 mm depth within the 2.5A and M0.4A coral cores (Table 1), which equates to reasonable growth rates of 14-17 mm/y over the post-earthquake interval (with the core-top set to May 2009). At the 2.5A site, the depth of the Ba/Ca-assigned earthquake event within the coral cores aligns with the base of a distinctive green-brown discolouration, distinctive high-density bands, and a shift to higher mean Ba/Ca (Supplementary Figs S3, S4). We note that the juvenile coral M0.4A-3 grew more slowly after the earthquake (59 mm) compared to the other three M0.4A corals analysed by Gagan et al. (2015), where a step-change decrease in skeletal $\delta^{13}C$ due to coseismic subsidence occurs at 82-86 mm depth within the cores.

The primary goal of our study is to examine broad geochemical changes before and after the 2005 earthquake, thus basic age models are suitable for application to the ~9-year coral records. To quantify the post-earthquake geochemical response, averages were calculated for the coral growth intervals before (2000-2004.9) and after the earthquake (2005.25 to 2009) at each site. We performed t-tests to determine the significance of any post-earthquake geochemical shift using pre- and post-earthquake averages based on 4-5 years of coral growth (Supplementary Table 1). The t-test calculations exclude elevated Ba/Ca and Mn/Ca values that occur within (or immediately below) skeleton surrounded by live coral tissue at the time of collection. Specifically, at site 1.8A we see significantly elevated Ba/Ca values proximal to the tissue layer (Supplementary Fig. S7), which is consistent with previous studies of coral Ba/Ca (10-fold higher below tissue layer, Lewis et al. 2018). Additionally, the t-test analysis examines long-term shifts in geochemical records and does not include the Y/Ca records for corals 2.5A-1, 2.5A-3 and 1.8A-6 as they show transient increases with the earthquake.

Acknowledgements

We thank Dr Heri Harjono at the Indonesian Institute of Sciences (LIPI) for essential administrative and logistical support in Sumatra under LIPI research permit 3564/IV/KS/2009 and Kementerian Negara Riset dan Teknologi (RISTEK) research permit 04/TKPIPA/FRP/SM/IV/2009. We are grateful to the captain and crew of our research vessel, the *Andalas*, for support for the coral drilling in Nias, and Les Kinsley, Steve Eggins, Joe Cali and Joan Cowley for laboratory support at RSES, ANU. We thank Jennie Mallela and Michele Lavigne for helpful discussions on an early draft of the manuscript. This work was supported by Australian Research Council Discovery grants DP0663227, DP110101161 and DP180103762 to M.K.G., W.S.H. and D.H.N., and an American Australian Association Postdoctoral Fellowship to S.M.S. S.M.S. also acknowledges financial support provided by the Welsh Government and Higher Education Funding Council for Wales through the Sêr Cymru National Research Network for Low Carbon, Energy and Environment.

Author contributions

S.M.S.: conceptualization, methodology, fieldwork, laboratory analysis, visualisation, writing – original draft, writing – review and editing, data curation. M.K.G.: conceptualization, methodology, fieldwork, resources, visualisation, writing – original draft, writing – review and editing, project administration, data curation. D.H.N.: fieldwork, resources, visualisation, writing – review and editing. B.W.S.: fieldwork, resources, writing – review and editing. H.R.: fieldwork, writing – review and editing. D.P.: underwater coral drilling, writing – review and editing. I.S.: underwater coral drilling, writing – review and editing. H.S-G.: investigation, visualisation, writing – review and editing. W.S.H.: resources, project administration, writing – review and editing.

References

1. Abram, N. J. *et al.* Coral reef death during the 1997 Indian Ocean Dipole linked to Indonesian wildfires. *Science* **301**, 952–955 (2003).
2. Albert, S., Udy, J., Baines, G. & McDougall, D. Dramatic tectonic uplift of fringing reefs on Ranongga Is., Solomon Islands. *Coral Reefs* **26**, 983–983 (2007).
3. Alibert, C. *et al.* Source of trace element variability in Great Barrier Reef corals affected by the Burdekin flood plumes. *Geochim. Cosmochim. Acta* **67**, 231–246 (2003).
4. Aronson, R. B., Precht, W. F., Macintyre, I. G. & Toth, L. T. Catastrophe and the life span of coral reefs. *Ecology* **93**, 303–313 (2012).
5. Briggs, R. W. *et al.* Deformation and slip along the Sunda megathrust in the great 2005 Nias-Simeulue earthquake. *Science* **311**, 1897–1901 (2006).
6. Cortés, J., Soto, R. & Jiménez, C. Earthquake associated mortality of intertidal and coral reef organisms (Caribbean of Costa Rica). In *Proceedings of the Seventh International Coral Reef Symposium* (ed. Richmond, R. H.) 235–240 (University of Guam Press, 1993).
7. Chlieh, M. *et al.* Coseismic slip and afterslip of the great M_w 9.15 Sumatra–Andaman earthquake of 2004. *Bull. Seismol. Soc. Am.* **97**, S152–S173 (2007).
8. Chunga-Llauce, J. A. & Pacheco, A. S. Impacts of earthquakes and tsunamis on marine benthic communities: A review. *Mar. Environ. Res.* **171**, 105481; 10.1016/j.marenvres.2021.105481 (2021).
9. Dadson, S. J. *et al.* Earthquake-triggered increase in sediment delivery from an active mountain belt. *Geology* **32**, 733–736 (2004).
10. Druffel, E. R. M. Geochemistry of corals: proxies of past ocean chemistry, ocean circulation, and climate. *Proc. Natl. Acad. Sci.* **94**, 8354–8361 (1997).
11. Eggins, S. M., Kinsley, L. P. J. & Shelley, J. M. G. Deposition and element fractionation processes during atmospheric pressure laser sampling for analysis by ICP-MS. *Appl. Surf. Sci.* **127–129**, 278–286 (1998).
12. Erftemeijer, P. L. A., Riegl, B., Hoeksema, B. W. & Todd, P. A. Environmental impacts of dredging and other sediment disturbances on corals: A review. *Mar. Poll. Bull.* **64**, 1737–1765 (2012).
13. Esslemont, G., Russell, R. A. & Maher, W. A. Coral record of harbour dredging: Townsville, Australia. *J. Mar. Syst.* **52**, 51–64 (2004).
14. Fallon, S. J., McCulloch, M. T., van Woesik, R. & Sinclair, D. J. Corals at their latitudinal limits: laser ablation trace element systematics in *Porites* from Shirigai Bay, Japan. *Earth Planet. Sci. Lett.* **172**, 221–238 (1999).
15. Fallon, S. J., White, J. C. & McCulloch, M. T. *Porites* corals as recorders of mining and environmental impacts: Misima Island, Papua New Guinea. *Geochim. Cosmochim. Acta* **66**, 45–62 (2002).
16. Fleitmann, D. *et al.* East African soil erosion recorded in a 300 year old coral colony from Kenya. *Geophys. Res. Lett.* **34**, L04401; 10.1029/2006GL028525 (2007).
17. Foster, R. *et al. Tsunami and Earthquake Damage to Coral Reefs of Aceh, Indonesia* (Reef Check Foundation, 2006).
18. Gagan, M. K., Chivas, A. R. & Isdale, P. J. Timing coral-based climatic histories using ^{13}C enrichments driven by synchronized spawning. *Geology* **24**, 1009–1012 (1996).
19. Gagan, M. K. *et al.* (2000). New views of tropical paleoclimates from corals. *Quat. Sci. Rev.* **19**, 45–64 (2000).

20. Gagan, M. K. *et al.* Coral $^{13}C/^{12}C$ records of vertical seafloor displacement during megathrust earthquakes west of Sumatra. *Earth Planet. Sci. Lett.* **432**, 461–471 (2015).

21. Haldar, D., Raman, M. & Dwivedi, R. M. Tsunami - a jolt for phytoplankton variability in the seas around Andaman Islands: a case study using IRS P4-OCM data. *Indian Journal of Geo-Marine Sciences* **42**, 437–447 (2013).

22. Hill, E. M. *et al.* The 2010 M_w 7.8 Mentawai earthquake: Very shallow source of a rare tsunami earthquake determined from tsunami field survey and near-field GPS data. *J. Geophys. Res.* **117**, B06402; 1029/2012JB009159 (2012).

23. Horii, T., Ueki, I. & Ando, K. Coastal upwelling events, salinity stratification, and barrier layer observed along the southwestern coast of Sumatra. *J. Geophys. Res.* **125**, e2020JC016287; 10.1029/2020JC016287 (2020).

24. Hovius, N. *et al.* Prolonged seismically induced erosion and the mass balance of a large earthquake. *Earth Planet. Sci. Lett.* **304**, 347–355 (2011).

25. Inoue, M. *et al.* Evaluation of Mn and Fe in coral skeletons (*Porites* spp.) as proxies for sediment loading and reconstruction of 50 yrs of land use on Ishigaki Island, Japan. *Coral Reefs* **33,** 363–373 (2014).

26. Ito, S., Yamazaki, A., Nishimura, Y., Yulianto, E. & Watanabe, T. Coral geochemical signals and growth responses to coseismic uplift during the great Sumatran megathrust earthquakes of 2004 and 2005. *Geochim. Cosmochim. Acta* **273**, 257–274 (2020).

27. Jaffe, B. E. *et al.* Northwest Sumatra and offshore islands field survey after the December 2004 Indian Ocean tsunami. *Earthquake Spectra* **22**, S105–S135; 10.1193/1.2207724 (2006).

28. Jupiter, S. *et al.* Linkages between coral assemblages and coral proxies of terrestrial exposure along a cross-shelf gradient on the southern Great Barrier Reef. *Coral Reefs* **27,** 887–903 (2008).

29. Kalnejais, L. H., Martin, W. R. & Bothner, M. H. The release of dissolved nutrients and metals from coastal sediments due to resuspension. *Mar. Chem.* **121**, 224–235 (2010).

30. Kasper-Zubillaga, J. J., Rosales-Hoz, L. & Bernal, J. P. Rare earth elements in corals from the Isla de Sacrificios Reef, Veracruz, Mexico, *Chemie Der Erde-Geochemistry* **70,** 55–60 (2010).

31. Keith, S. A., Baird, A. H., Hughes, T. P., Madin, J. S. & Connolly, S. R. Faunal breaks and species composition of Indo-Pacific corals: the role of plate tectonics, environment and habitat distribution. *Proc. R. Soc. B: Biol. Sci.* **280**, 20130818; 10.1098/rspb.2013.0818 (2013).

32. Konca, A. O. *et al.* Partial rupture of a locked patch of the Sumatra megathrust during the 2007 earthquake sequence. *Nature* **456**, 631–635 (2008).

33. Leonard, N. D. *et al.* High resolution geochemical analysis of massive *Porites spp*. corals from the Wet Tropics, Great Barrier Reef: rare earth elements, yttrium and barium as indicators of terrigenous input. *Mar. Poll. Bull.* **149**, 110634; 10.1016/j.marpolbul.2019.110634 (2019).

34. Leprieur, F. *et al.* Plate tectonics drive tropical reef biodiversity dynamics. *Nat. Comm.* **7**, 11461; 10.1038/ncomms11461 (2016).

35. Lewis, S. E., Shields, G. A., Kamber, B. S. & Lough, J. M. A multi-trace element coral record of land-use changes in the Burdekin River catchment, NE Australia. *Palaeogeogr. Palaeoclimatol. Palaeoecol.* **246,** 471–487 (2007).

36. Lewis, S. E. *et al.* An assessment of an environmental gradient using coral geochemical records, Whitsunday Islands, Great Barrier Reef, Australia. *Mar. Poll. Bull.* **65**, 306–319 (2012).

37. Lewis, S. E. *et al.* A critical evaluation of coral Ba/Ca, Mn/Ca and Y/Ca ratios as indicators of terrestrial input: New data from the Great Barrier Reef, Australia. *Geochim. Cosmochim. Acta* **237**, 131–154 (2018).

38. Lough, J. M. & Barnes, D. J. Several centuries of variation in skeletal extension, density and calcification in massive *Porites* colonies from the Great Barrier Reef: a proxy for seawater temperature and a background of variability against which to identify unnatural change. *J. Exp. Mar. Biol. Ecol.* **211**, 29–67 (1997).

39. McAdoo, B. G. *et al.* Solomon Islands tsunami, one year later. *Eos Trans. AGU* **89**, 10.1029/2008EO180001 (2008).

40. McCulloch, M. *et al.* Coral record of increased sediment flux to the inner Great Barrier Reef since European settlement. *Nature* **421**, 727–730 (2003).

41. Meltzner, A. J. *et al.* Coral evidence for earthquake recurrence and an A.D. 1390–1455 cluster at the south

end of the 2004 Aceh-Andaman rupture. *J. Geophys. Res.* **115**, B10402; 10.1029/2010JB007499 (2010).

42. Meltzner, A. J. *et al.* Persistant termini of 2004- and 2005-like ruptures of the Sunda megathrust. *J. Geophys. Res.* **117**, B04405; 10.1029/2011JB008888 (2012).

43. Meltzner, A. J. *et al.* Time-varying interseismic strain rates and similar seismic ruptures on the Nias–Simeulue patch of the Sunda megathrust. *Quat. Sci. Rev.* **122**, 258–281 (2015).

44. Mihaljevic, M., Korpanty, C., Renema, W., Welsh, K. & Pandolfi, J. M. Identifying patterns and drivers of coral diversity in the Central Indo-Pacific marine biodiversity hotspot. *Paleobiology* **43**, 343–364 (2017).

45. Moyer, R. P., Grottoli, A. G. & Olesik, J. W. A multiproxy record of terrestrial inputs to the coastal ocean using minor and trace elements (Ba/Ca, Mn/Ca, Y/Ca) and carbon isotopes ($\delta^{13}C$, $\Delta^{14}C$) in a nearshore coral from Puerto Rico. *Paleoceanography* **27**, PA3205; 10.1029/2011PA002249 (2012).

46. Natawidjaja, D. H. *et al.* Paleogeodetic records of seismic and aseismic subduction from central Sumatran microatolls, Indonesia, *J. Geophys. Res.*, **109**, B04306; 10.1029/2003JB002398 (2004).

47. Natawidjaja, D. H. *et al.* Source parameters of the great Sumatran megathrust earthquakes of 1797 and 1833 inferred from coral microatolls. *J. Geophys. Res.* **111**, B06403; 10.1029/2005JB004025 (2006).

48. Natawidjaja, D. H. et al. Interseismic deformation above the Sunda Megathrust recorded in coral microatolls of the Mentawai islands, West Sumatra. *J. Geophys. Res.* **112**, B02404; 10.1029/2006JB004450 (2007).

49. Ogilvie, B. G. & Mitchell, S. F. Does sediment resuspension have persistent effects on phytoplankton? experimental studies in three shallow lakes. *Freshw. Biol.* **40**, 51–63 (1998).

50. Philibosian, B. *et al.* Rupture and variable coupling behaviour of the Mentawai segment of the Sunda megathrust during the supercycle culmination of 1797 to 1833. *J. Geophys. Res.* **119**, 7258–7287 (2014).

51. Philibosian, B. *et al.* Earthquake supercycles on the Mentawai segment of the Sunda megathrust in the seventeenth century and earlier. *J. Geophys. Res.* **122**, 642–676 (2017).

52. Saha, N., Webb, G. E. & Zhao, J.-x. Coral skeletal geochemistry as a monitor of inshore water quality. *Sci. Total. Environ.* **566–567**, 652–684 (2016).

53. Saha, N., Webb, G. E., Zhao, J.-x., Leonard, N. D. & Nguyen, A. D. Influence of marine biochemical cycles on seasonal variation of Ba/Ca in the near-shore coral *Cyphastrea*, Rat Island, southern Great Barrier Reef. *Chem. Geol.* **499**, 71–83 (2018).

54. Saha, N. *et al.* Seasonal to decadal scale influence of environmental drivers on Ba/Ca and Y/Ca in coral aragonite from the southern Great Barrier Reef. *Sci. Total Environ.* **639**, 1099–1109 (2018).

55. Saji, N. H., Goswami, B. N., Vinayachandran, P. H. & Yamagata, T. A dipole mode in the tropical Indian Ocean. *Nature* **401**, 360–363 (1999).

56. Sarangi, R. K. Impact assessment of the Japanese tsunami on ocean-surface chlorophyll concentration using MODIS-Aqua data. *J. Appl. Remote Sens.* **6**, 063539; 10.1117/1.JRS.6.063539 (2012).

57. Sayani, H. R. *et al.* Reproducibility of coral Mn/Ca-based wind reconstructions at Kiritimati Island and Butaritari Atoll. *Geochem. Geophys. Geosyst.* **22**, e2020GC00939; 10.1029/2020GC009398 (2021).

58. Searle, M. P. Co-seismic uplift of coral reefs along the western Andaman Islands during the December 26th 2004 earthquake. *Coral Reefs* **25**, 2-2 (2006).

59. Sepulveda, R. D. & Valdivia, N. Localised effects of a mega-disturbance: spatiotemporal responses of intertidal sandy shore communities to the 2010 Chilean earthquake. *Plos One* **11**, e0157910; 10.1371/journal.pone.0157910 (2016).

60. Siringoringo, R. M., Hadi, T. A., Sari, N. W. P., Abrar, M. & Munasik. Distribution and community structure of coral reefs in the west coast of Sumatra, Indonesia. *Ilmu Kelautan: Indonesian Jour. Mar. Sci.* **24**, 51–60 (2019).

61. Siringoringo, R. M., Putra, R. D., Abrar, M., Sari, N. W. P. & Giyanto. Coral reef damage and recovery related to a massive earthquake (March 2005) in Nias Island, Indonesia. *AACL Bioflux* **14,** (2021).

62. Shen, G. T. *et al.* Paleochemistry of manganese in corals from the Galapagos Islands. *Coral Reefs* **10**, 91–100 (1991).

63. Sieh, K. *et al.* Earthquake supercycles inferred from sea-level changes recorded in the corals of West Sumatra. *Science* **322**, 1674–678 (2008).

64. Sinclair, D. J. Non-river flood barium signals in the skeletons of corals from coastal Queensland, Australia.

Earth Planet. Sci. Lett. **237**, 354–369 (2005).

65. Sinclair, D. J., Kinsley, L. P. J. & McCulloch, M. T. High resolution analysis of trace elements in corals by laser ablation ICP-MS. *Geochim. Cosmochim. Acta* **62**, 1889–1901 (1998).
66. Stoddart, D. R. Catastrophic damage to coral reef communities by earthquake. *Nature* **239**, 51–52 (1972).
67. Tanzil, J. T. I. *et al.* Multi-colony coral skeletal Ba/Ca from Singapore's turbid urban reefs: Relationship with contemporaneous in-situ seawater parameters. *Geochim. Cosmochim. Acta* **250**, 191–208 (2019).
68. Taylor, F. W. *et al.* Rupture across arc segment and plate boundaries in the 1 April 2007 Solomons earthquake. *Nat. Geosci.* **1**, 253–257 (2008).
69. Taylor, F. W. Earthquakes and emergence or submergence of coral reefs. In *Encyclopedia of Modern Coral Reefs: structure, form and process* (ed. Hopley, D.) 327–333 (Springer, 2011).
70. Tengberg, A., Almroth-Rosell, E. & Hall, P. O. J. Resuspension and its effects on organic carbon recycling and nutrient exchange in coastal sediments: In situ measurements using new experimental technology. *J. Exp. Mar. Biol. Ecol.* **285–286**, 119–142 (2003).
71. Thomsen, M. S. *et al.* Cascading impacts of earthquakes and extreme heatwaves have destroyed populations of an iconic marine foundation species. *Divers. Distrib.* **27**, 2369–2383 (2021).
72. van Woesik, R. Earthquake effects on a coral reef in Japan. *Coral Reefs* **15**, 224–224 (1996).
73. Walther, B. D., Kingsford, M. J. & McCulloch, M. T. Environmental records from Great Barrier Reef corals: inshore versus offshore drivers. *Plos One* **8**, e77091; 10.1371/journal.pone.0077091 (2013).
74. Wyndham, T., McCulloch, M. T., Fallon, S. J. & Alibert, C. High-resolution coral records of rare earth elements in coastal seawater: biogeochemical cycling and a new environmental proxy. *Geochim. Cosmochim. Acta* **68**, 2067–2080 (2004).
75. Yamazaki, A. *et al.* Seasonal variations in the nitrogen isotope composition of Okinotori coral in the tropical western Pacific: A new proxy for marine nitrate dynamics. *J. Geophys. Res.* **116**, G04005; 10.1029/2011JG001697 (2011).
76. Zachariasen, J., Sieh, K., Taylor, F. W., Edwards, R. L. & Hantoro, W. S. Submergence and uplift associated with the giant 1833 Sumatran subduction earthquake: Evidence from coral microatolls. *J. Geophys. Res.* **104**, 895–919 (1999).

Supplementary Information

Supplementary Figures

Figure S1: Underwater photos of *Porites sp.* corals drilled at sites NS09-2.5A, NS09-1.8A and NS09-M0.4A.

Figure S2: X-radiographs for coral drill-cores NS09-1.8A-2, NS09-1.8A-5 and NS09-1.8A-6.

Figure S3: Photo, X-radiograph and age model for coral drill-core NS09-2.5A-1.

Figure S4: Photo, X-radiograph and age model for coral drill-core NS09-2.5A-3.

Figure S5: X-radiograph and age model for coral drill-core NS09-M0.4A-3.

Figure S6: LA-ICP-MS Ba/Ca, Mn/Ca and Y/Ca data profiles for NS09-2.5A-1 and NS09-2.5A-3.

Figure S7: LA-ICP-MS Ba/Ca, Mn/Ca and Y/Ca data profiles for NS09-1.8A-2, NS09-1.8A-5 and NS09-1.8A-6.

Figure S8: LA-ICP-MS Ba/Ca, Mn/Ca and Y/Ca data profiles for NS09-M0.4A-3.

Supplementary Data

Table S1: T-test results for pre- and post-earthquake elemental ratios in the Nias corals.

Supplementary References

Supplementary Figures

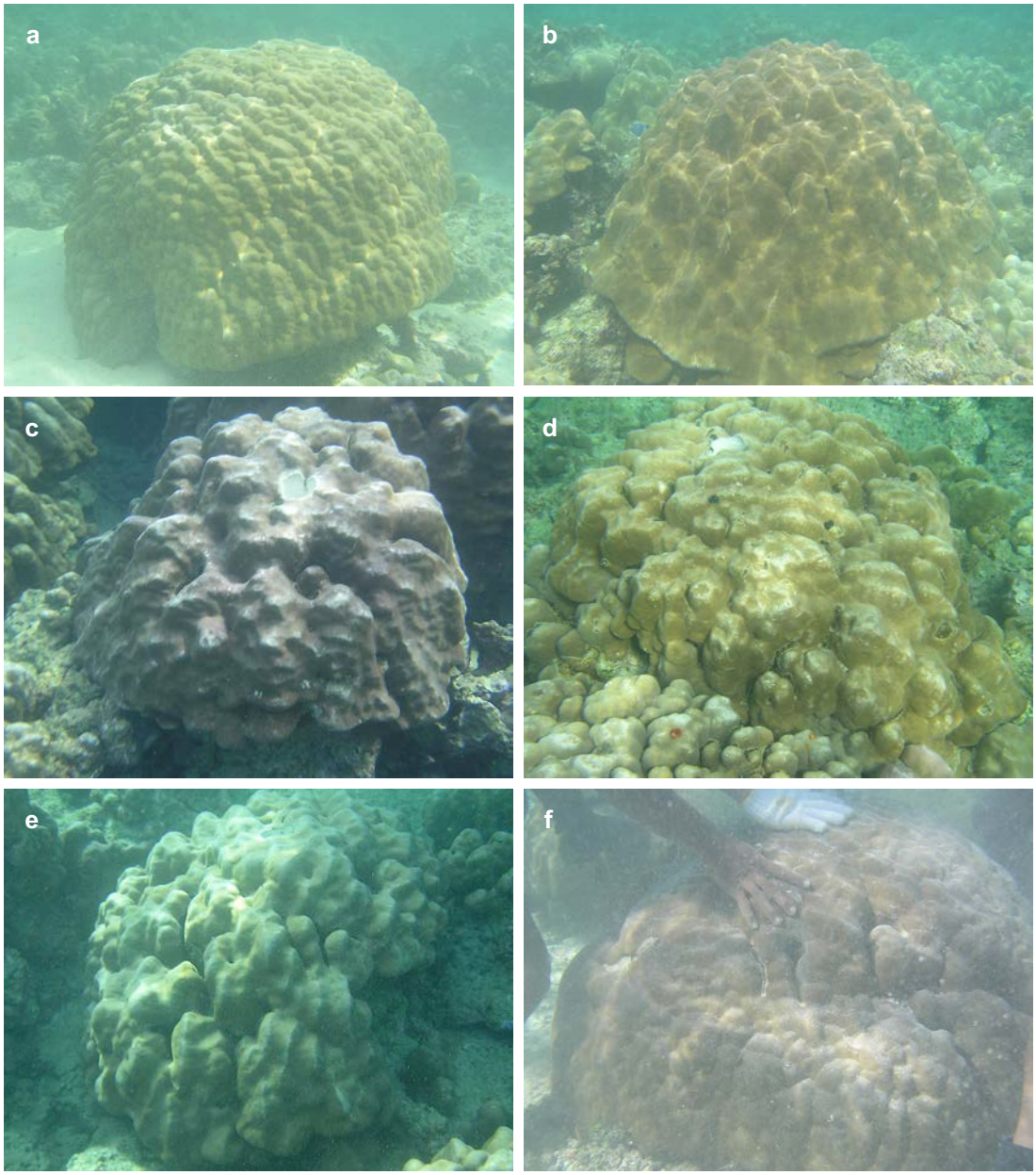

Figure S1 | Underwater photos of *Porites sp.* corals drilled at sites NS09-2.5A, NS09-1.8A and NS09-M0.4A. Corals 2.5A-1 (**a**) and 2.5A-3 (**b**) drilled on 20 May 2009 in turbid water in the shallow platform reef lagoon created by 2.5 m coseismic uplift west of Lahewa Harbour. Corals 1.8A-2 (**c**), 1.8A-5 (**d**) and 1.8A-6 (**e**) drilled on 24-25 May 2009 along the fringing reef at Hilimakora Island with 1.8 m coseismic uplift. Coral M0.4A-3 (**f**) drilled on 27 May 2009 in the offshore fringing reef lagoon at Sarangbaung Island with 0.4 m coseismic subsidence.

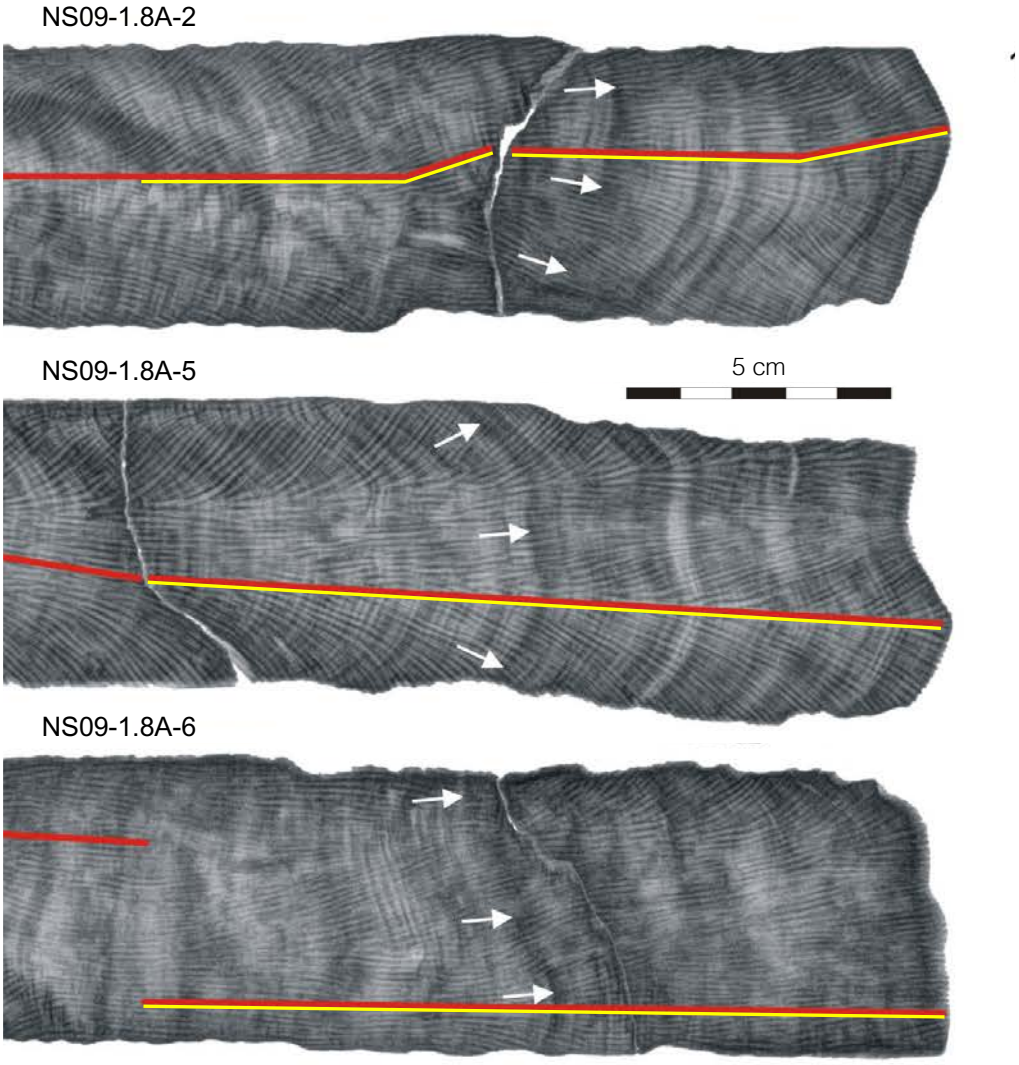

Figure S2 | X-ray positive images (dark = higher density) of *Porites sp.* corals NS09-1.8A-2, NS09-1.8A-5 and NS09-1.8A-6 (adapted from Gagan et al. 2015). The corals were drilled underwater adjacent to the fringing reef at Hilimakora Island that was raised by 1.8 m during the 28 March 2005 earthquake (Briggs et al. 2006). Arrows in each core mark the depth of a slight increase in skeletal density following the earthquake. Red lines show sampling transects used for stable isotope analysis (Gagan et al. 2015). Yellow lines show the ~150-mm lengths of the LA-ICP-MS sampling tracks positioned alongside the stable isotope transects.

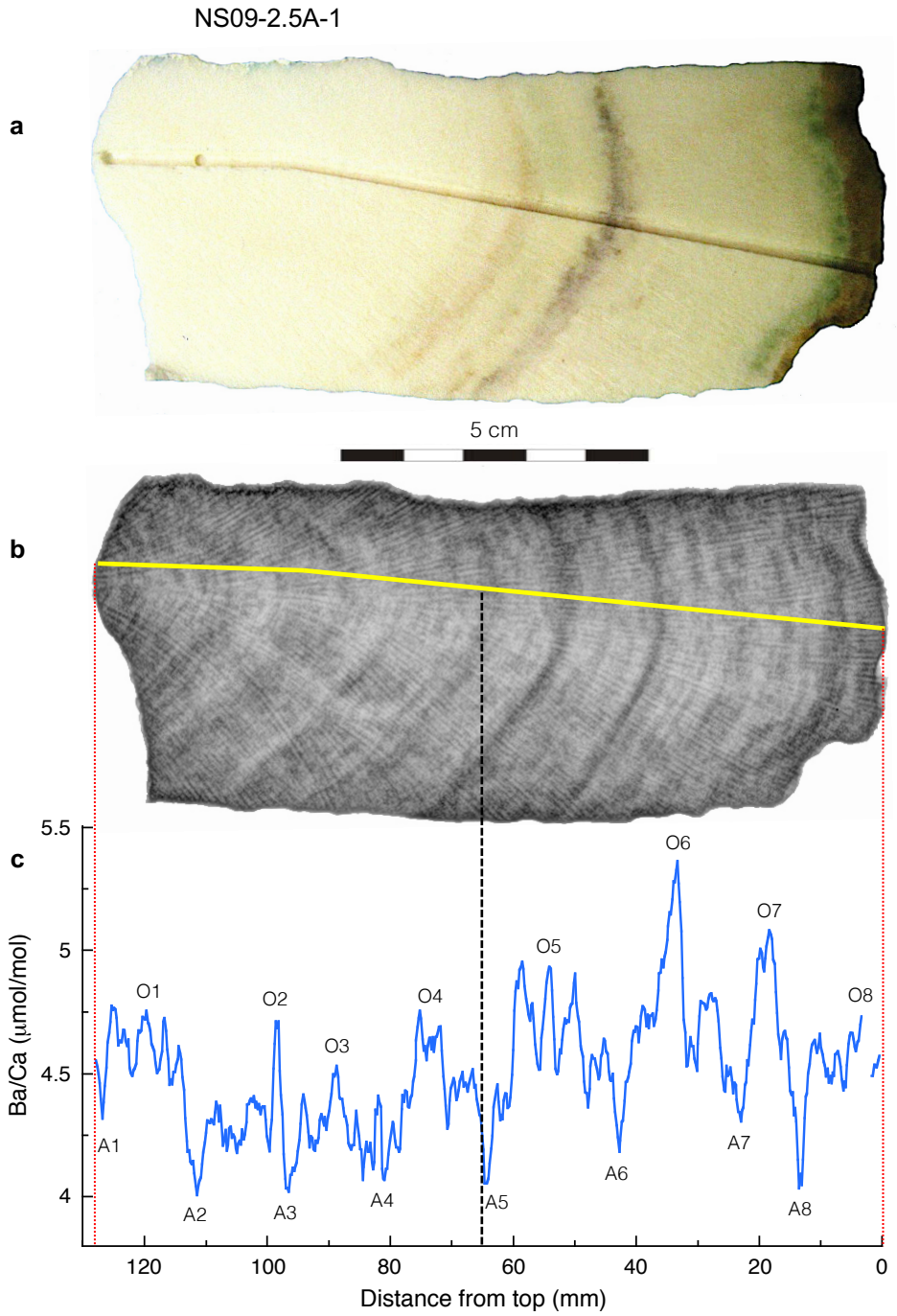

Figure S3 | Photo, X-radiograph and age model for coral drill-core NS09-2.5A-1. (**a**) Photo of the coral slab for *Porites sp.* coral 2.5A-1 drilled underwater in the shallow lagoon of the raised reef west of Lahewa Harbour. The coral was raised by 2.5 m during the 28 March 2005 earthquake (Briggs et al. 2006) and shows post-earthquake skeletal discolouration and distinctive green-brown banding**.** (**b**) X-ray positive image (dark = higher density) of the coral slab. Yellow line shows the 128-mm length of the LA-ICP-MS sampling track. (**c**) Seasonal cycles of skeletal Ba/Ca (5-pt running means) used to develop the age model for coral 2.5A-1. The chronology is based on linear interpolation between tie-points assigned to mid-April (low Ba/Ca) and mid-October (high Ba/Ca) (see Methods). Black dashed line marks approximate depth to the March 2005 earthquake.

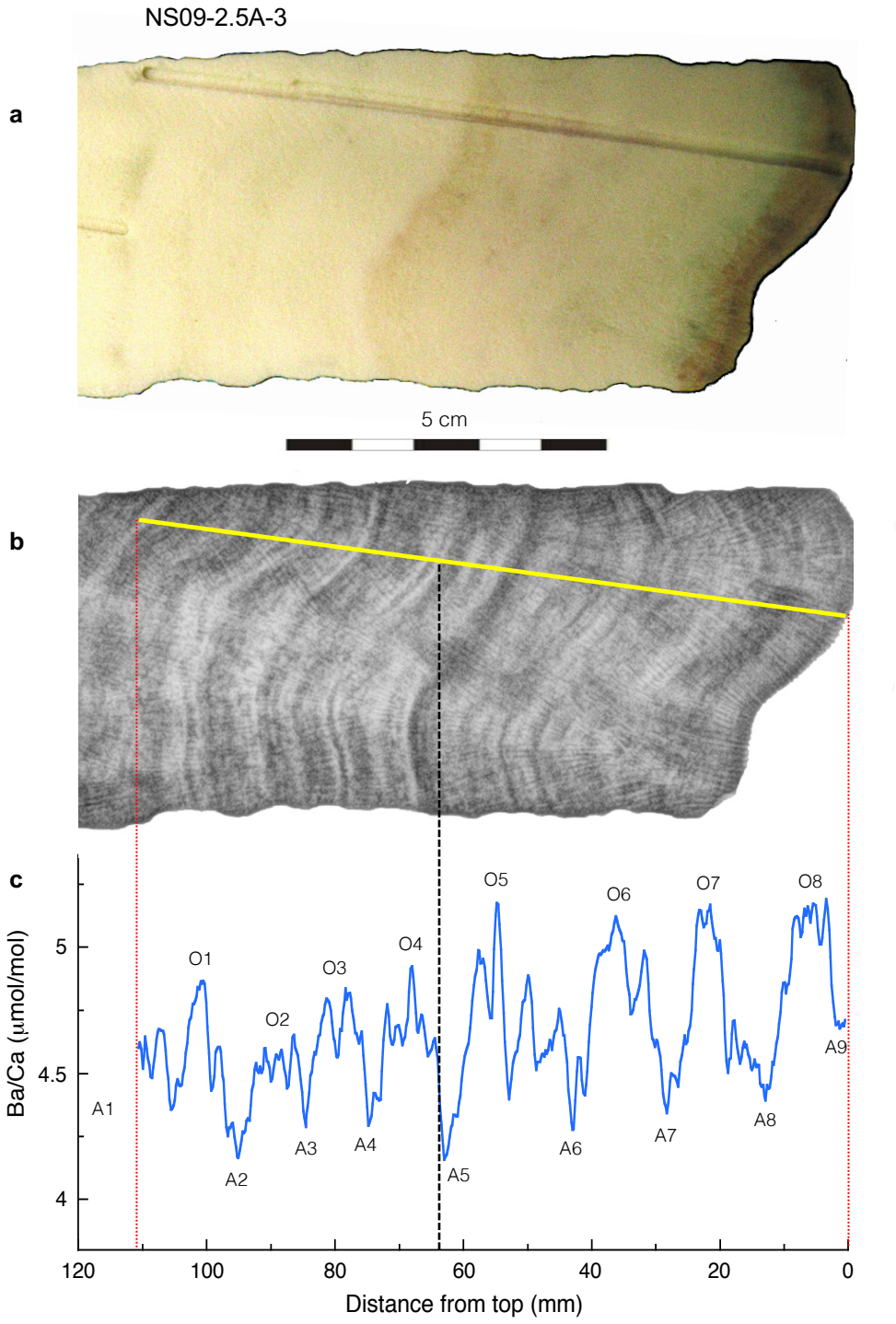

Figure S4 | Photo, X-radiograph and age model for coral drill-core NS09-2.5A-3. (**a**) Photo of the coral slab for *Porites sp.* coral 2.5A-3 drilled underwater in the shallow lagoon of the raised reef west of Lahewa Harbour. The coral was raised by 2.5 m during the 28 March 2005 earthquake (Briggs et al. 2006) and shows post-earthquake skeletal discolouration**.** (**b**) X-ray positive image (dark = higher density) of the coral slab. Yellow line shows the 111-mm length of the LA-ICP-MS sampling track. (**c**) Seasonal cycles of skeletal Ba/Ca (5-pt running means) used to develop the age model for coral 2.5A-3. The chronology is based on linear interpolation between tie-points assigned to mid-April (low Ba/Ca) and mid-October (high Ba/Ca) (see Methods). Black dashed line marks approximate depth to the March 2005 earthquake.

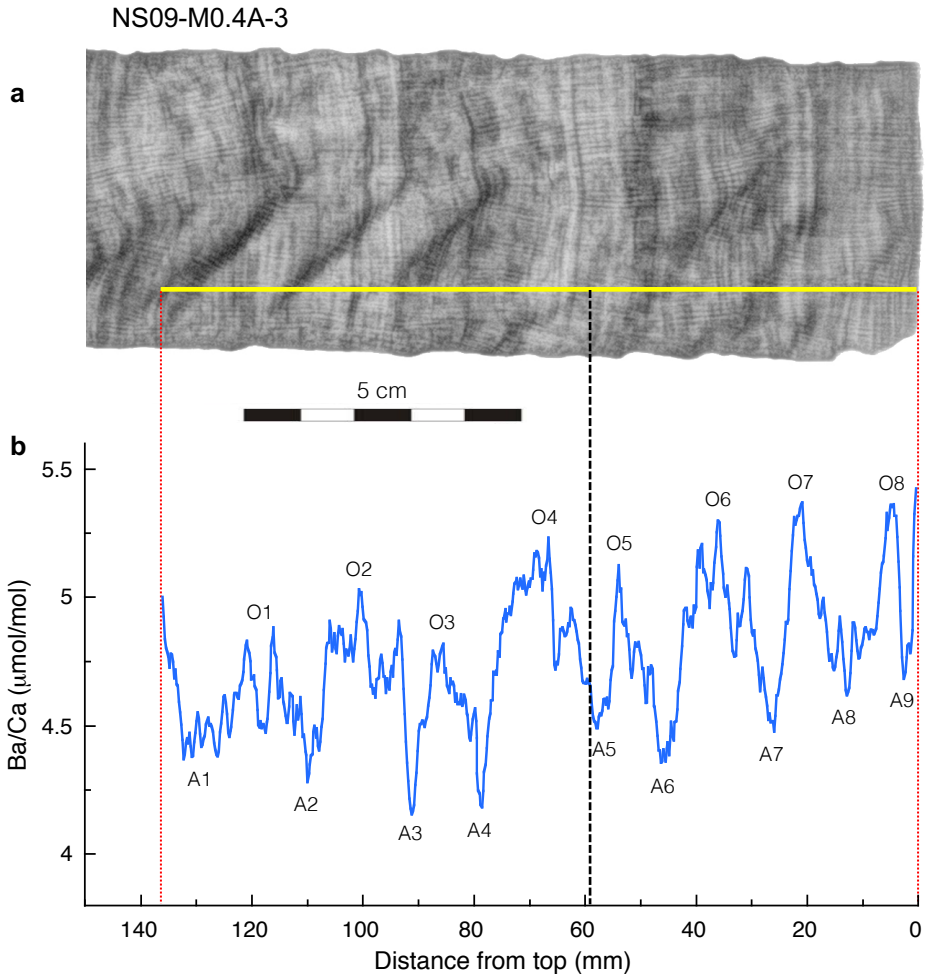

Figure S5 | X-radiograph and age model for coral drill-core NS09-M0.4A-3. (**a**) X-ray positive image (dark = higher density) of *Porites sp.* coral M0.4A-3 drilled underwater in the lagoon of the submerged reef at Sarangbaung Island. The coral subsided by 0.4 m during the 28 March 2005 earthquake (Briggs et al. 2006). Yellow line shows the 137-mm length of the LA-ICP-MS sampling track. (**b**) Seasonal cycles of skeletal Ba/Ca (5-pt running means) used to develop the age model for coral M0.4A-3. The chronology is based on linear interpolation between tie-points assigned to mid-April (low Ba/Ca) and mid-October (high Ba/Ca) (see Methods). Black dashed line marks approximate depth to the March 2005 earthquake.

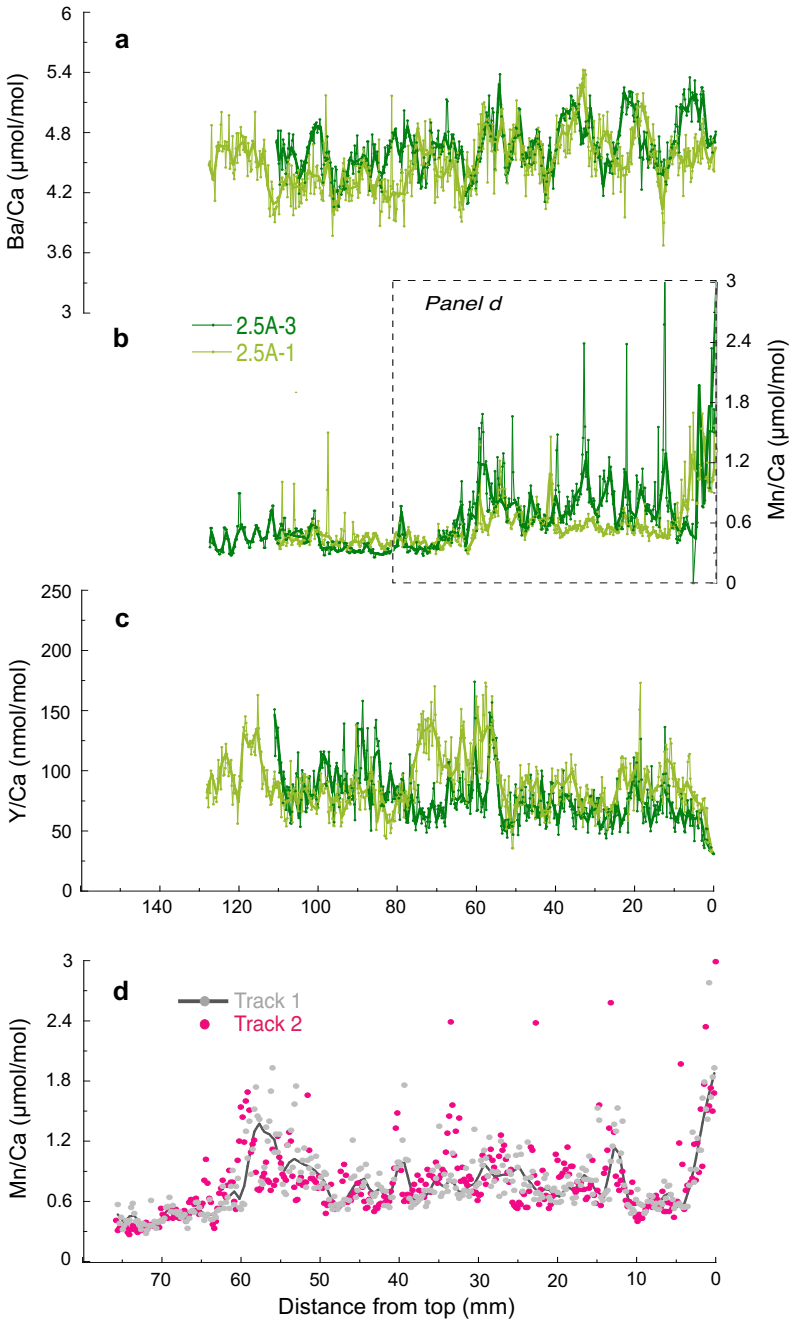

Figure S6 | LA-ICP-MS Ba/Ca, Mn/Ca and Y/Ca data profiles for drill-cores NS09-2.5A-1 and NS09-2.5A-3. (**a-c**) Raw Ba/Ca, Mn/Ca and Y/Ca data (thin lines) and 10-pt running means (thick lines). (**d**) Replicate analysis of Mn/Ca along two sampling tracks in core 2.5A-1. Mn/Ca data for track 1 were acquired with the major trace element analysis protocol (for Ba, Mn), using a 50 x 500 µm laser spot size. Track 2 Mn/Ca data were acquired with the trace element protocol (for Y/Ca), using a 100 x 500 µm laser spot size (following Wyndham et al. 2004). The good replication of the two records shows that the LA-ICP-MS methods are robust, and suggests that Mn signals are lattice bound within the coral aragonite.

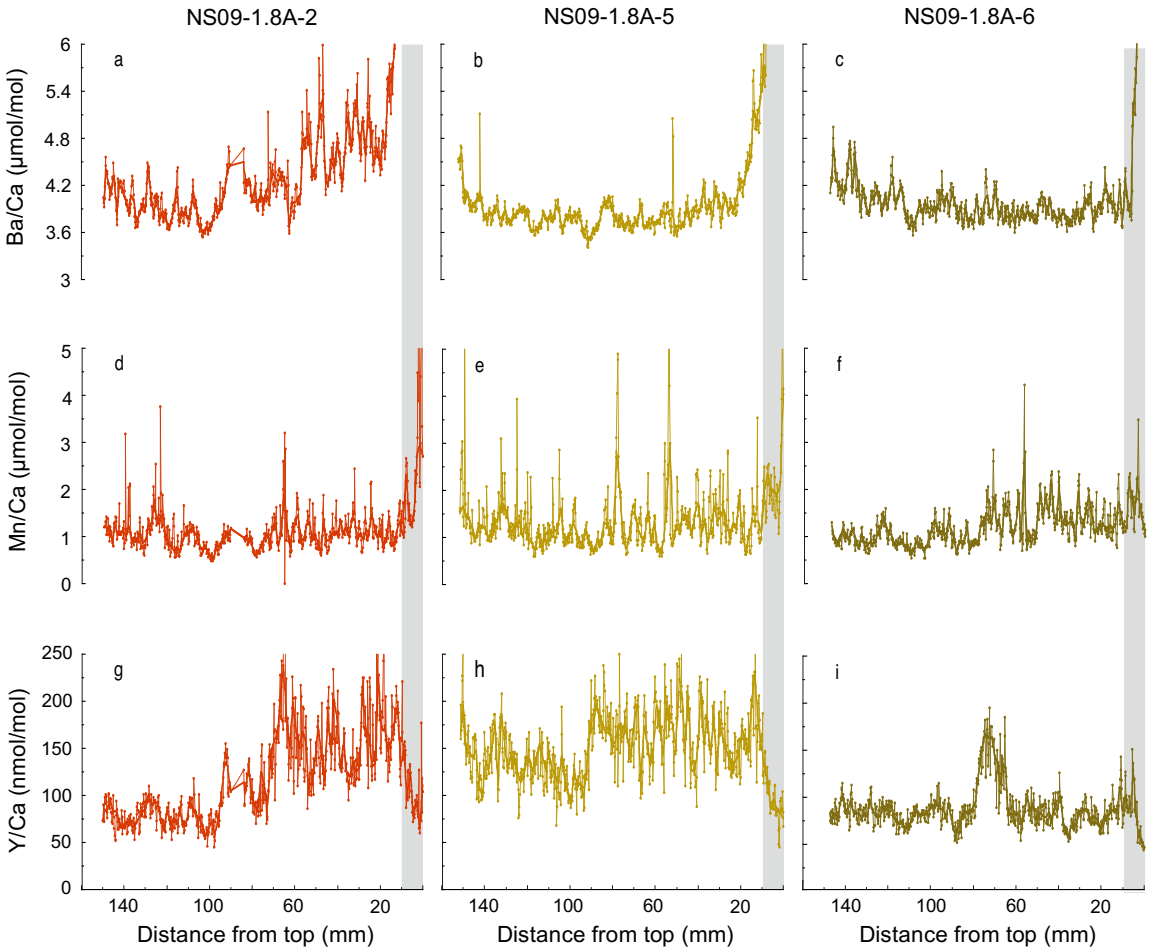

Figure S7 | LA-ICP-MS Ba/Ca, Mn/Ca and Y/Ca data profiles for drill-cores NS09-1.8A-2, NS09-1.8A-5 and NS09-1.8A-6. (**a-c**) Comparison of raw Ba/Ca data (thin lines) and 10-pt running means (thick lines) for the three site 1.8A corals. (**d-f**) As above, but comparison of Mn/Ca. (**g-i**) As above, but comparison of Y/Ca. Grey shadng in each panel represents the tissue layer.

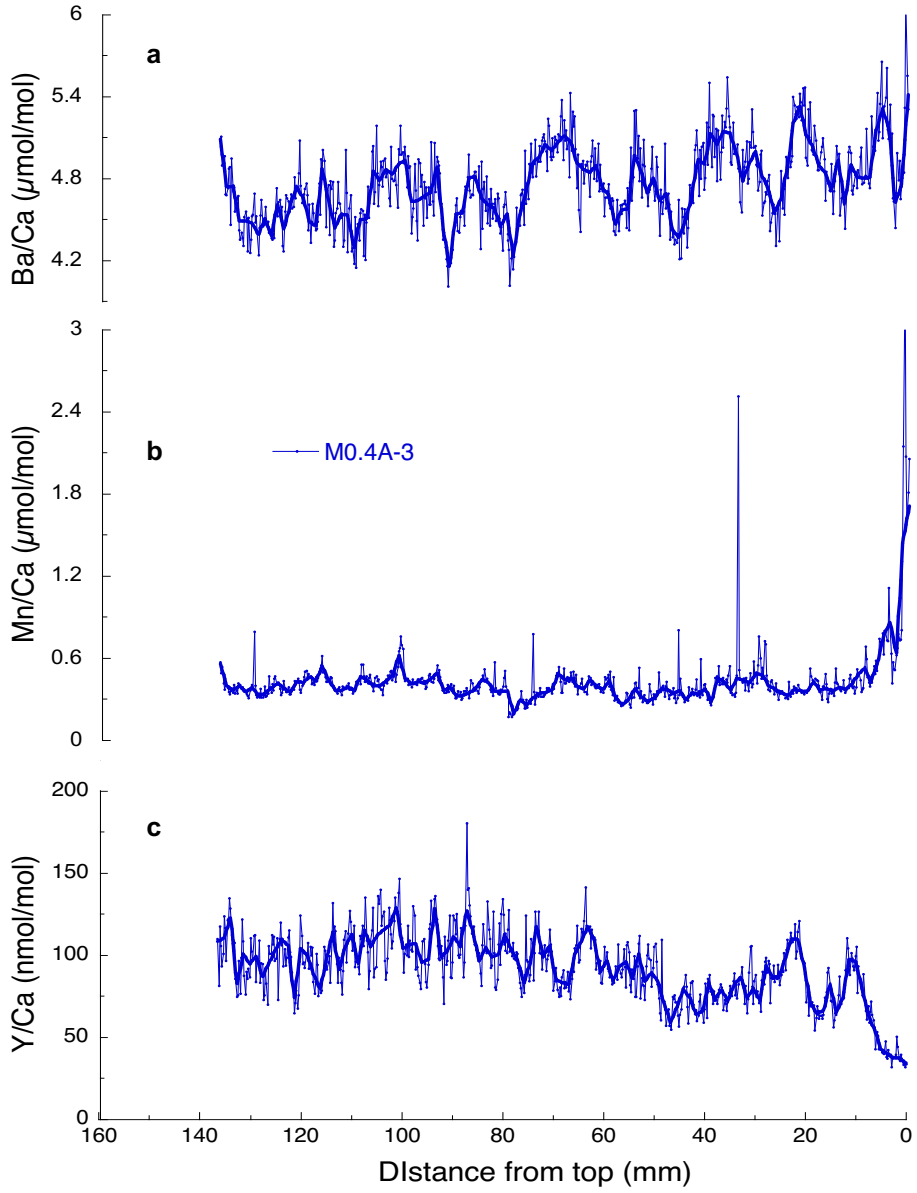

Figure S8 | LA-ICP-MS Ba/Ca, Mn/Ca and Y/Ca data profiles for drill-core NS09-M0.4A-3. (**a-c**) Raw Ba/Ca, Mn/Ca and Y/Ca data (thin lines) and 10-pt running means (thick lines).

Supplementary Data

Table S1. T-test results for pre- and post-earthquake elemental ratios in the Nias corals. A t-test p-value <0.0001 indicates a significant difference between pre- and post-earthquake mean elemental ratio values. Differences highlighted in blue and orange represent a post-earthquake increase and decrease, respectively. Data within the tissue layer were not included in post-earthquake statistics for Ba and Mn.

	Mn/Ca (µmol/mol)							
Coral ID	**Pre-EQ Mean**	**Pre-EQ SD**	**Pre-EQ SE**	**Post-EQ Mean**	**Post-EQ SD**	**Post-EQ SE**	**ΔEQ**	**T-Test p-value**
2.5A-1	0.39	0.10	0.01	0.82	0.34	0.02	0.43	**<0.0001**
2.5A-3	0.44	0.12	0.01	0.64	0.22	0.01	0.20	**<0.0001**
1.8A-2	0.98	0.37	0.02	1.15	0.39	0.02	0.17	**<0.0001**
1.8A-5	1.24	0.53	0.03	1.42	0.75	0.04	0.18	**<0.0001**
1.8A-6	0.97	0.21	0.01	1.42	0.42	0.02	0.45	**<0.0001**
M0.4A-3	0.40	0.08	0.00	0.41	0.17	0.01	0.01	
	Y/Ca (nmol/mol)							
Coral ID	**Pre-EQ Mean**	**Pre-EQ SD**	**Pre-EQ SE**	**Post-EQ Mean**	**Post-EQ SD**	**Post-EQ SE**	**ΔEQ**	**T-Test p-value**
1.8A-2	84.9	21.4	1.2	158.4	44.4	2.6	73.5	**<0.0001**
1.8A-5	139.2	32.0	1.8	163.8	32.4	1.8	24.6	**<0.0001**
	Ba/Ca (µmol/mol)							
Coral ID	**Pre-EQ Mean**	**Pre-EQ SD**	**Pre-EQ SE**	**Post-EQ Mean**	**Post-EQ SD**	**Post-EQ SE**	**ΔEQ**	**T-Test p-value**
2.5A-1	4.39	0.25	0.02	4.63	0.29	0.02	0.24	**<0.0001**
2.5A-3	4.56	0.20	0.01	4.74	0.28	0.02	0.18	**<0.0001**
1.8A-2	3.2	0.8	0.04	6.5	2.5	0.17	3.35	**<0.0001**
1.8A-5	2.76	0.67	0.04	2.89	0.67	0.04	0.13	
1.8A-6	3.39	0.78	0.04	2.98	0.51	0.03	-0.41	**<0.0001**
M0.4A-3	4.67	0.26	0.01	4.85	0.28	0.02	0.18	**<0.0001**

Supplementary References

Briggs, R. W. *et al.* Deformation and slip along the Sunda megathrust in the great 2005 Nias-Simeulue earthquake. *Science* **311**, 1897–1901 (2006).

Gagan, M. K. *et al.* Coral $^{13}C/^{12}C$ records of vertical seafloor displacement during megathrust earthquakes west of Sumatra. *Earth Planet. Sci. Lett.* **432**, 461–471 (2015).

Wyndham, T., McCulloch, M. T., Fallon, S. J. & Alibert, C. High-resolution coral records of rare earth elements in coastal seawater: biogeochemical cycling and a new environmental proxy. *Geochim. Cosmochim. Acta* **68**, 2067–2080 (2004).